Mon. Not. R. Astron. Soc. **000**, 1–20 (2005) Printed 5 February 2008 (MN LATEX style file v1.4)

Wave Excitation in Three-Dimensional Disks by External Potential

Hang Zhang[1,2⋆] and Dong Lai[2,3⋆]
[1] *Department of Physics, Nanjing Normal University, Nanjing, JS 210097, P.R. China*
[2] *Department of Astronomy, Cornell University, Ithaca, NY 14853, USA*
[3] *National Astronomical Observatories, Chinese Academy of Sciences, Beijing, 100012, China*

Accepted ????. Received ?????; in original form ?????

ABSTRACT

We study the excitation of density and bending waves and the associated angular momentum transfer in gaseous disks with finite thickness by a rotating external potential. The disk is assumed to be isothermal in the vertical direction and has no self-gravity. The disk perturbations are decomposed into different modes, each characterized by the azimuthal index m and the vertical index n, which specifies the nodal number of the density perturbation along the disk normal direction. The $n = 0$ modes correspond to the two-dimensional density waves previously studied by Goldreich & Tremaine and others. In a three-dimensional disk, waves can be excited at both Lindblad resonances (for modes with $n = 0, 1, 2, \cdots$) and vertical resonances (for the $n \geq 1$ modes only). The torque on the disk is positive for waves excited at outer Linblad/vertical resonances and negative at inner Lindblad/vertical resonances. While the $n = 0$ modes are evanescent around corotation, the $n \geq 1$ modes can propagate into the corotation region where they are damped and deposit their angular momenta. We have derived analytical expressions for the amplitudes of different wave modes excited at Lindblad and/or vertical resonances and the resulting torques on the disk. It is found that for $n \geq 1$, angular momentum transfer through vertical resonances is much more efficient than Lindblad resonances. This implies that in some situations (e.g., a circumstellar disk perturbed by a planet in an inclined orbit), vertical resonances may be an important channel of angular momentum transfer between the disk and the external potential. We have also derived new formulae for the angular momentum deposition at corotation and studied wave excitations at disk boundaries.

Key words: accretion, accretion discs - hydrodynamics - waves - binaries: general - planetary systems

1 INTRODUCTION

Gravitational interaction between a gaseous disk and an an external body plays an important role in many astrophysical systems, including protoplanetary disks, binary stars and spiral galaxies. The external potential generates disturbances in the disk, shaping the structure and evolution of the disk, and these, in turn, influence the dynamics of the external object itself. In a classic paper, Goldreich & Tremaine (1979; hereafter GT) studied density wave excitation by an external potential in a two-dimensional disk and gave the formulation of angular momentum transport rate or torque at Lindblad and corotation resonances for disks with or without self-gravity (see also Goldreich & Tremaine 1978; Lin & Papaloizou 1979). Since then, numerous extensions and applications of their theory have appeared in the literature. For example, Shu, Yuan & Lissauer (1985) studied the effect of nonlinearities of the waves on the resonant torque. Meyer-Vernet & Sicardy (1987) examined the transfer of angular momentum in a disk subjected to perturbations at Lindblad resonance under various physical conditions.

⋆ Email: zhanghang@njnu.edu.cn; dong@astro.cornell.edu

Artymowicz (1993) derived a generalized torque formula which is useful for large azimuthal numbers. The saturation of the corotation resonance were investigated in detail by many authors (e.g., Balmforth & Korycansky 2001; Ogilvie & Lubow 2003). Korycansky & Pollack (1993) performed numerical calculations of the torques. Applications of the GT theory were mostly focused on disk-satellite interactions, including the eccentricity and inclination evolution of the satellite's orbit (e.g., Goldreich & Tremaine 1980; Ward 1988; Goldreich & Sari 2003) and protoplanet migration in the Solar Nebula (e.g., Ward 1986, 1997; Masset & Papaloizou 2003).

A number of studies have been devoted to the three-dimensional (3D) responses of a disk to an external potential. Lubow (1981) analyzed wave generation by tidal force at the vertical resonance in an isothermal accretion disk and investigated the possibility that the resonantly driven waves can maintain a self-sustained accretion. Ogilvie (2002) generalized Lubow's analysis to non-isothermal disks and also considered nonlinear effects. Lubow & Pringle (1993) studied the propagation property of 3D axisymmetric waves in disks, and Bate et al. (2002) examined the excitation, propagation and dissipation of axisymmetric waves. Wave excitation at Lindblad resonances in thermally stratified disks was investigated by Lubow & Ogilvie (1998) using shearing sheet model. Takeuchi & Miyama (1998) studied wave generation at vertical resonances in isothermal disks by external gravity. Tanaka, Takeuchi & Ward (2002) investigated the corotation and Lindblad torque brought forth from the 3D interaction between a planet and an isothermal gaseous disk. The excitation of bending waves was studied by Papaloizou & Lin (1995) and Terquem (1998) in disks without resonances. Artymowicz (1994), Ward & Hahn (2003) and Tanaka & Ward (2004) investigated many aspects of resonance-driven bending waves.

Despite all these fruitful researches, a unified description and analysis of wave excitation in 3D disks by external potentials are still desirable. This is the purpose of our paper. As a first step, we only consider linear theory. Our treatment allows for Lindblad, corotation and vertical resonances to be described within the same theoretical framework, and in the meantime, density waves and bending waves to be handled in an unified manner. By taking advantage of Fourier-Hermite expansion, different modes of perturbation for locally isothermal disks are well organized and a second-order differential equation for individual mode is attained (see Tanaka, Takeuchi & Ward 2002). In order to treat it mathematically, the derived equation which appears monstrous is pruned under different situations for those modes with the highest order of magnitude. Then, following the standard technique used by Goldreich & Tremaine (1979), the simplified equations are solved and analytic expressions for the waves excited at various locations and associated angular momentum transfer rates are calculated.

Our paper is organized as follows. The derivation of the basic equations describing the response of a disk to an external potential are briefly presented in §2. The assumptions underlying our formulation are also specified there. In §3 we examine the dispersion relation for free waves and various resonances which may exist in the disk. Wave modes are organized according to the azimuthal index m and the vertical index n, with $n = 0$ corresponding to the modes in a 2D disk. In §4 we study Lindblad resonances. §4.1 deals with the $n \neq 1$ cases, where the solutions pertaining to the waves excited at the resonances are found and the angular momentum transports by such waves are calculated. The $n = 1$ case is treated separately in §4.2, because in this case the Lindblad resonance coincides with the vertical resonance for a Keplerian disk. In §5 we study wave excitation and angular momentum transport at vertical resonances for general n. Corotation resonances are examined in §6, where it is necessary to treat the $n \geq 1$ and $n = 0$ cases separately. In §7 we study wave excitation at disk boundaries. We discuss the effects of various assumptions adopted in our treatment in §8 and summarize our main result in §9. Appendix A contains general solutions of disk perturbations away from resonances, and Appendix B gives a specific example of angular momentum flow in the disk: wave excitation at a Lindblad or vertical resonance, followed by wave propagation, and finally wave damping at corotation.

2 BASIC EQUATIONS

We consider a geometrically thin gas disk and adopt cylindrical coordinates (r, θ, z). The unperturbed disk has velocity $\mathbf{v}_0 = (0, r\Omega, 0)$, where the angular velocity $\Omega = \Omega(r)$ is taken to be a function of r alone. The disk is assumed to be isothermal in the vertical direction and non-self-gravitating. The equation of hydrostatic equilibrium (for $z \ll r$) reads

$$\frac{dp_0}{dz} = -\rho_0 \Omega_\perp^2 z. \tag{1}$$

Thus the vertical density profile is given by

$$\rho_0(r, z) = \frac{\sigma}{\sqrt{2\pi}h} \exp(-Z^2/2), \quad \text{with} \quad Z = z/h \tag{2}$$

where $h = h(r) = c/\Omega_\perp$ is the disk scale height, $c = c(r) = \sqrt{p_0/\rho_0}$ is the isothermal sound speed, $\sigma = \sigma(r) = \int dz\, \rho_0$ is the surface density, and $\Omega_\perp$ is the vertical oscillation frequency of the disk.

We now consider perturbation of the disk driven by an external potential ϕ. The linear perturbation equations read

$$\frac{\partial \mathbf{u}}{\partial t} + (\mathbf{v}_0 \cdot \nabla)\mathbf{u} + (\mathbf{u} \cdot \nabla)\mathbf{v}_0 = -\frac{1}{\rho_0}\nabla \delta P + \frac{\delta \rho}{\rho_0^2}\nabla p_0 - \nabla \phi, \tag{3}$$

$$\frac{\partial \rho}{\partial t} + \nabla \cdot (\rho_0 \mathbf{u} + \mathbf{v}_0 \delta\rho) = 0, \tag{4}$$

where $\delta\rho$, δP and $\mathbf{u} = \delta\mathbf{v}$ are the (Eulerian) perturbations of density, pressure and velocity, respectively. Without loss of generality, each perturbation variable X and the external potential ϕ are assumed to have the form of a normal mode in θ and t

$$X(r, \theta, z, t) = X(r, z) \exp(im\theta - i\omega t), \tag{5}$$

where m is a nonnegative integer and consequently, ω is allowed to be either positive or negative, corresponding to the prograde or retrograde wave, respectively. Note that only the real part of the perturbation has physical meaning and we will not write out explicitly the dependence on m and ω for the amplitude $X(r, z)$ and other related quantities in this paper. The equation for adiabatic perturbations is $dP/dt = c_s^2 d\rho/dt$, where c_s is the adiabatic sound speed. This yields

$$-i\tilde{\omega}(\delta P - c_s^2 \delta\rho) = c_s^2 \rho_0 \mathbf{u} \cdot \mathbf{A}, \tag{6}$$

where

$$\tilde{\omega} = \omega - m\Omega \tag{7}$$

is the "Doppler-shifted" frequency, and

$$\mathbf{A} = \frac{\nabla \rho_0}{\rho_0} - \frac{\nabla p_0}{c_s^2 \rho_0} \tag{8}$$

is the Schwarzschild discriminant vector. In general, $|A_r| \sim 1/r$ may be neglected compared to $|A_z| \sim 1/h$ for thin disks ($h \ll r$). In the following, we will also assume $A_z = 0$, i.e., the disk is neutrally stratified in the vertical direction. This amounts to assuming $c_s = c$ (i.e., the perturbations are assumed isothermal). Equation (6) then becomes $\delta P = c^2 \delta\rho$. Introducing the enthalpy perturbation

$$\eta = \delta p / \rho_0, \tag{9}$$

Equations (3) and (4) reduce to †

$$-i\tilde{\omega} u_r - 2\Omega u_\theta = -\frac{\partial}{\partial r}(\eta + \phi), \tag{10}$$

$$-i\tilde{\omega} u_\theta + \frac{\kappa^2}{2\Omega} u_r = -\frac{im}{r}(\eta + \phi), \tag{11}$$

$$-i\tilde{\omega} u_z = -\frac{\partial}{\partial z}(\eta + \phi), \tag{12}$$

$$-i\tilde{\omega}\frac{\rho_0}{c^2}\eta + \frac{1}{r}\frac{\partial}{\partial r}(r\rho_0 u_r) + \frac{im}{r}\rho_0 u_\theta + \frac{\partial}{\partial z}(\rho_0 u_z) = 0. \tag{13}$$

Here κ is the epicyclic frequency, defined by

$$\kappa^2 = \frac{2\Omega}{r}\frac{d}{dr}(r^2\Omega). \tag{14}$$

In this paper we will consider cold, (Newtonian) Keplerian disks, for which the three characteristic frequencies, $\Omega, \Omega_\perp$ and κ, are identical and equal to the Keplerian frequency $\Omega_K = (GM/r^3)^{1/2}$. However, we continue to use different notations $(\Omega, \Omega_\perp, \kappa)$ for them in our treatment below when possible so that the physical origins of various terms are clear.

Following Tanaka et al. (2002) and Takeuchi & Miyama (1998) (see also Okazaki et al. 1987; Kato 2001), we expand the perturbations with Hermite polynomials H_n:

$$\begin{aligned} \begin{bmatrix} \phi(r,z) \\ \eta(r,z) \\ u_r(r,z) \\ u_\theta(r,z) \end{bmatrix} &= \sum_n \begin{bmatrix} \phi_n(r) \\ \eta_n(r) \\ u_{rn}(r) \\ u_{\theta n}(r) \end{bmatrix} H_n(Z), \\ u_z(r,z) &= \sum_n u_{zn}(r) H_n'(Z), \end{aligned} \tag{15}$$

where $H_n' = dH_n/dZ$. The Hermite polynomials $H_n(Z) \equiv (-1)^n e^{Z^2/2} d^n(e^{-Z^2/2})/dZ^n$ satisfy the following equations:

$$H_n'' - ZH_n' + nH_n = 0, \tag{16}$$

$$H_n' = nH_{n-1}, \tag{17}$$

† On the right-hand-side of eq. (10), we have dropped the term $2(d\ln c/dr)\eta$. In effect, we assume c is constant in radius. Relaxing this assumption does not change the results of the paper. See §8 for a discussion.

$$ZH_n = H_{n+1} + nH_{n-1}, \tag{18}$$

$$\int_{-\infty}^{\infty} \exp(-Z^2/2) H_n H_{n'} dZ = \sqrt{2\pi}\, n!\, \delta_{nn'}. \tag{19}$$

We note that any complete set of functions can be used as the basis of the expansion. For an example, Lubow(1981) used Taylor series in the expansion of vertical variable. However, choosing the Hermite polynomials as the basis set, as we shall see, greatly simplifies the mathematics involved, since they are eigenmodes in variable z for locally isothermal disks with a constant scale height h and quasi-eigenmodes for disks with a small radial variation of h. Note that since $H_1 = Z$, $H_2 = Z^2 - 1$, the $n = 1$ mode coincides with the bending mode studied by Papaloizou & Lin (1995) (who considered disks with no resonance), and the $n = 2$ mode is similar to the mode studied by Lubow (1981).

With the expansion in (15), the fluid equations (13) become

$$-i\tilde{\omega} u_{rn} - 2\Omega u_{\theta n} = -\frac{d}{dr} w_n + \frac{n\mu}{r} w_n + \frac{(n+1)(n+2)\mu}{r} w_{n+2}, \tag{20}$$

$$-i\tilde{\omega} u_{\theta n} + \frac{\kappa^2}{2\Omega} u_{rn} = -\frac{im}{r} w_n, \tag{21}$$

$$-i\tilde{\omega} u_{zn} = -w_n/h, \tag{22}$$

$$-i\tilde{\omega}\frac{\eta_n}{c^2} + \left(\frac{d}{dr}\ln r\sigma + \frac{n\mu}{r}\right) u_{rn} + \frac{\mu}{r} u_{r,n-2} + \frac{d}{dr} u_{rn} + \frac{im}{r} u_{\theta n} - \frac{n}{h} u_{zn} = 0, \tag{23}$$

where

$$w_n \equiv \eta_n + \phi_n, \tag{24}$$

and

$$\mu \equiv \frac{d\ln h}{d\ln r}. \tag{25}$$

Eliminating $u_{\theta n}$ and u_{zn} from eqs. (20)-(23), we have

$$\frac{dw_n}{dr} = \frac{2m\Omega}{r\tilde{\omega}} w_n - \frac{D}{\tilde{\omega}} i u_{rn} + \frac{\mu}{r}[n w_n + (n+1)(n+2) w_{n+2}], \tag{26}$$

$$\frac{du_{rn}}{dr} = -\left[\frac{d\ln(r\sigma)}{dr} + \frac{m\kappa^2}{2r\Omega\tilde{\omega}}\right] u_{rn} + \frac{1}{i\tilde{\omega}}\left(\frac{m^2}{r^2} + \frac{n}{h^2}\right) w_n + \frac{i\tilde{\omega}}{c^2}\eta_n - \frac{\mu}{r}(n u_{rn} + u_{r,n-2}), \tag{27}$$

where we have defined

$$D \equiv \kappa^2 - \tilde{\omega}^2 = \kappa^2 - (\omega - m\Omega)^2. \tag{28}$$

Finally, we eliminate u_{rn} to obtain a single second-order differential equation for η_n [see eq. (21) of Tanaka et al. 2002] ‡:

$$\begin{aligned}
&\left[\frac{d^2}{dr^2} + \left(\frac{d}{dr}\ln\frac{r\sigma}{D}\right)\frac{d}{dr} - \frac{2m\Omega}{r\tilde{\omega}}\left(\frac{d}{dr}\ln\frac{\Omega\sigma}{D}\right) - \frac{m^2}{r^2} - \frac{D(\tilde{\omega}^2 - n\Omega_\perp^2)}{c^2\tilde{\omega}^2}\right] w_n \\
&+\frac{\mu}{r}\left[\left(\frac{d}{dr} - \frac{2m\Omega}{r\tilde{\omega}}\right) w_{n-2} + n\left(\frac{d}{dr}\ln\frac{D}{\sigma} - \frac{4m\Omega}{r\tilde{\omega}}\right) w_n \right.\\
&\qquad \left. -(n+1)(n+2)\left(\frac{d}{dr} - \frac{d}{dr}\ln\frac{D}{\sigma} + \frac{2m\Omega}{r\tilde{\omega}}\right) w_{n+2}\right] \\
&-\frac{\mu^2}{r^2}\Big[(n-2) w_{n-2} + n(2n-1) w_n + n(n+1)(n+2) w_{n+2}\Big] = -\frac{D}{c^2}\phi_n.
\end{aligned} \tag{29}$$

Obviously, for $\mu = 0$, different n-modes are decoupled. But even for $\mu \neq 0$, approximate mode separation can still be achieved: When we focus on a particular n-mode, its excitation at the resonance is decoupled from the other n-modes (see Sects. 4-6), provided that the orders of magnitudes of $\eta_{n\pm2}$ and their derivatives are not much larger than η_n and $d\eta_n/dr$ — we shall adopt this assumption in remainder of this paper. Note that if $\eta_{n\pm2}$ is much larger than η_n, the coupling terms must be kept. In this case, the problem can be treated in a sequential way. After arranging the potential ϕ_n's in the order of their magnitudes, from large to small, we first treat the mode with the largest ϕ_n; in solving this "dominant" mode, the coupling terms involving the other "secondary" n-modes can be neglected. We then proceed to solve the next mode in the sequence: Here the coupling terms with the dominant mode may not be neglected, but since the dominant mode is already known, these

‡ On the left-hand-side of eq. (29), we have dropped the term $-r^{-1}(d\mu/dr)\,[n w_n + (n+1)(n+2) w_{n+2}]$. This term does not change the results of this paper. Also, for a Keplerian disk with c =constant, $h \propto r^{3/2}$ and $d\mu/dr = 0$. See §8 for a discussion.

coupling terms simply act as a "source" for the secondary mode and the torque formulae derived in the following sections (§§4-7) can be easily modified to account for the additional source.

In the absence of self-gravity, waves excited by external potential carry angular momentum by advective transport. The time averaged transfer rate of the z-component of angular momentum across a cylinder of radius r is given by (see Lynden-Bell & Kalnajs 1972; GT; Tanaka et al. 2002)

$$F(r) = \left\langle r^2 \int_{-\infty}^{\infty} dz \int_0^{2\pi} d\theta\, \rho_0(r,z) u_r(r,\theta,z,t) u_\theta(r,\theta,z,t) \right\rangle. \tag{30}$$

Note that a positive (negative) $F(r)$ implies angular momentum transfer outward (inward) in radius. Using $u_r(r,\theta,z,t) = \mathrm{Re}\,[u_{r\,n} H_n(Z) e^{i(m\theta-\omega t)}]$, $u_\theta(r,\theta,z,t) = \mathrm{Re}\,[u_{\theta\,n} H_n(Z) e^{i(m\theta-\omega t)}]$, and eqs. (2) and (19), we find that the angular momentum flux associated with the (n,m)-mode is

$$F_n(r) = n!\,\pi r^2 \sigma\, \mathrm{Re}\,(u_{r\,n} u^*_{\theta\,n}) \tag{31}$$

(recall that we do not explicitly write out the dependence on m). Using eqs. (20) and (21), this reduces to (see Tanaka et al. 2002)

$$F_n(r) = \frac{n!\,\pi m r \sigma}{D} \mathrm{Im}\left[w_n \frac{dw_n^*}{dr} - (n+1)(n+2)\frac{\mu}{r} w_n w_{n+2}^* \right], \tag{32}$$

where $w_n = \eta_n + \phi_n$. To simplify eq. (32) further, we shall carry out local averaging of $F_n(r)$ over a a scale much larger than the local wavelength $|k|^{-1}$ (see GT). As we see in the next sections, the perturbation η_n generated by the external potential ϕ_0 generally consists of a nonwave part $\bar{\eta}_n$ and a wave part $\tilde{\eta}_n$; thus $w_n = \phi_n + \bar{\eta}_n + \tilde{\eta}_n$. The cross term between $(\phi_n + \bar{\eta}_n)$ and $\tilde{\eta}_n$ in eq. (32) can be neglected after the averaging. The coupling term ($\propto w_n w_{n+2}^*$) between different modes can also be dropped because of the radial averaging and $|w_{n+2}| \lesssim |w_n|$ (see above). Thus only the wave-like perturbation carries angular momentum, and eq. (32) simplifies to

$$F_n(r) \approx \frac{n!\,\pi m r \sigma}{D} \mathrm{Im}\left(\tilde{\eta}_n \frac{d\tilde{\eta}_n^*}{dr} \right). \tag{33}$$

In §§4-6, we will use eq. (32) or (33) to calculate the angular momentum transfer by waves excited or dissipated at various resonances.

3 DISPERSION RELATION AND RESONANCES

Before proceeding to study wave excitations, it is useful to consider local free wave solution of the form

$$\eta_n \propto \exp\left[i \int^r k(s) ds \right]. \tag{34}$$

For $|kr| \gg 1$, from the eq. (29), in the absence of the external potential, we find (see Okazaki et al. 1987; Kato 2001)

$$(\tilde{\omega}^2 - \kappa^2)(\tilde{\omega}^2 - n\Omega_\perp^2)/\tilde{\omega}^2 = k^2 c^2, \tag{35}$$

where we have used $h = c/\Omega_\perp \ll r$ (thin disk), and $m, n \ll r/h$ — we will be concerned with such m, n throughout this paper. Obviously, for $n = 0$ we recover the standard density-wave dispersion relation for 2D disks without self-gravity. In Appendix A, we discuss general WKB solutions of eq. (29).

At this point it is useful to consider the special resonant locations in the disk. These can be recognized by investigating the singular points and turning points of eq. (29) or by examining the characteristics of the dispersion relation (35). For $\omega > 0$, the resonant radii are

(i) Lindblad resonances (LRs), where $D = 0$ or $\tilde{\omega}^2 = \kappa^2$, including outer Lindblad resonance (OLR) at $\tilde{\omega} = \kappa$ and inner Lindblad resonance (ILR) at $\tilde{\omega} = -\kappa$. The LRs are apparent singularities of eq. (29) — we can see this from (26) and (27) that the wave equations are well-behaved and all physical quantities are finite at $D = 0$. The LRs are turning points at which wave trains are reflected or generated. Note that the ILR exists only for $m \geq 2$.

(ii) Corotation resonance (CR), where $\tilde{\omega} = 0$. In general, the CR is a (regular) singular point of eq. (29), except in the special case of $n = 0$ and $d(\Omega\sigma/\kappa^2)/dr = 0$ at corotation. Some physical quantities (e.g., azimuthal velocity perturbation) are divergent at corotation. Physically, this sigularity signifies that a steady emission or absorption of wave action may occur there. Note that no CR exists for $m = 0$.

(iii) Vertical resonances (VRs), where $\tilde{\omega}^2 = n\Omega_\perp^2$ (with $n \geq 1$), including outer vertical resonance (OVR) at $\tilde{\omega} = \sqrt{n}\Omega_\perp$ and inner vertical resonance (IVR) at $\tilde{\omega} = -\sqrt{n}\Omega_\perp$. The VRs are turning points of eq. (29). The IVR exists only for $m > \sqrt{n}$. Note that for Keplerian disks and $n = 1$, the LR and VR are degenerate.

For $\omega < 0$, a Lindblad resonance (LR) exists only for $m = 0$, where $\omega = -\kappa$, and a vertical resonance (VR) may exist for $m < \sqrt{n}$, but there is no corotation resonance in the disk.

From the dispersion relation we can identify the wave propagation zones for $\omega > 0$ (see Fig. 1 and Fig. 2): (1) For $n = 0$, the wave zone lies outside the OLR and ILR (i.e., $r > r_{OLR}$ and $r < r_{ILR}$); (2) For $n \geq 2$, the wave zones lie between ILR and OLR ($r_{ILR} < r < r_{OLR}$) and outside the IVR (if it exists) and OVR ($r < r_{IVR}$ and $r > r_{OVR}$); (3) For $n = 1$, waves can propagate everywhere.

The group velocity of the waves is given by

$$c_g \equiv \frac{d\omega}{dk} = \frac{kc^2}{\tilde{\omega}\left[1 - (\kappa/\tilde{\omega})^2(n\Omega_\perp^2/\tilde{\omega}^2)\right]}. \tag{36}$$

The relative sign of c_g and and the phase velocity $c_p = \omega/k$ is important for our study of wave excitations in §§4-7: For $\omega > 0$, positive (negative) c_g/c_p implies that trailing waves ($k > 0$) carry energy outward (inward), while leading waves ($k < 0$) carry energy inward (outward). The signs of c_g/c_p for different propagation regions are shown in Figs. 1-2. Note that for $n = 0$ and $n \geq 2$, $c_p \to \infty$ and $c_g \to 0$ as $k \to 0$ at the Linblad/vertical resonances. But for $n = 1$, we have

$$c_g = \frac{c\tilde{\omega}^2}{\tilde{\omega}^2 + \kappa^2}\,\mathrm{sgn}\,(-k\tilde{\omega}D). \tag{37}$$

Thus $|c_g| \to c/2$ at the Lindblad/vertical resonances [§].

4 LINDBLAD RESONANCES

We now study wave excitations near a Lindblad resonance (where $D = 0$). Equation (29) shows that different n-modes are generally coupled. However, when solving the equation for a given n-mode, the coupling terms can be neglected if $|\eta_n| \gtrsim |\eta_{n\pm2}|$. Note that in the vicinity of a Lindblad resonance, $|d\ln D/dr| \gg |d\ln\sigma/dr| \sim |d\ln\Omega/dr| \sim 1/r$. For a thin disk, if m and n not too large ($m, n \ll r/h$), the terms proportional to $c^{-2} \propto h^{-2}$ are the dominant non-singular terms. Keeping all the singular terms ($\propto D^{-1}$), we have

$$\left[\frac{d^2}{dr^2} - \left(\frac{d\ln D}{dr}\right)\frac{d}{dr} + \frac{2m\Omega}{r\tilde{\omega}}\left(\frac{d\ln D}{dr}\right) - \frac{D(\tilde{\omega}^2 - n\Omega_\perp^2)}{c^2\tilde{\omega}^2}\right]\eta_n$$
$$+\frac{\mu}{r}\left(\frac{d\ln D}{dr}\right)[n\eta_n + (n+1)(n+2)\eta_{n+2}] = \frac{d\ln D}{rdr}\psi_n - \frac{n\Omega_\perp^2 D}{c^2\tilde{\omega}^2}\phi_n, \tag{38}$$

where

$$\psi_n \equiv \left(r\frac{d}{dr} - \frac{2m\Omega}{\tilde{\omega}} - n\mu\right)\phi_n - \mu(n+1)(n+2)\phi_{n+2}. \tag{39}$$

Now the terms proportional to $(d\ln D/dr)\eta_n$ and $(d\ln D/dr)\eta_{n+2}$ can be dropped relative to the other terms (see Goldreich & Tremaine 1978)[¶], we then obtain

$$\left[\frac{d^2}{dr^2} - \left(\frac{d\ln D}{dr}\right)\frac{d}{dr} - \frac{D(\tilde{\omega}^2 - n\Omega_\perp^2)}{c^2\tilde{\omega}^2}\right]\eta_n = \frac{d\ln D}{rdr}\psi_n - \frac{n\Omega_\perp^2 D}{c^2\tilde{\omega}^2}\phi_n. \tag{40}$$

We now proceed to solve eq. (40). Note that besides its (apparent) singular behavior, the resonance point of $D = 0$ is a first-order turning (or transition) point when $n \neq 1$, and a second-order turning point when $n = 1$ for Keplerian disks. These two cases should be investigated separately.

4.1 $n \neq 1$ Mode

In the vicinity of the Lindblad resonance r_L, we change the independent variable from r to

$$x \equiv (r - r_L)/r_L \tag{41}$$

and replace D by $(r\,dD/dr)_{r_L}x + (r^2\,d^2D/dr^2)_{r_L}x^2/2$. For $|x| \ll 1$, eq. (40) becomes

[§] Of course, eqs. (35)-(36) are valid only away from the resonances, so the limiting values discussed here refer to the asymptotic limits as the resonances are approached.

[¶] To see this explicitly, we set $\eta_n = D^{1/2}y_n$ and reduce eq. (38) to the form $d^2y_n/dr^2 + f(r)y_n = \cdots$. We then find that the $(d\ln D/dr)\eta_n$ term in eq. (38) gives rise to a term $\propto (d\ln D/dr) \propto D^{-1}$ in $f(r)$, while the $d^2\eta_n/dr^2$ and $(d\ln D/dr)d\eta_n/dr$ terms in eq. (38) both contribute terms proportional to $(d\ln D/dr)^2 \propto D^{-2}$ in $f(r)$.

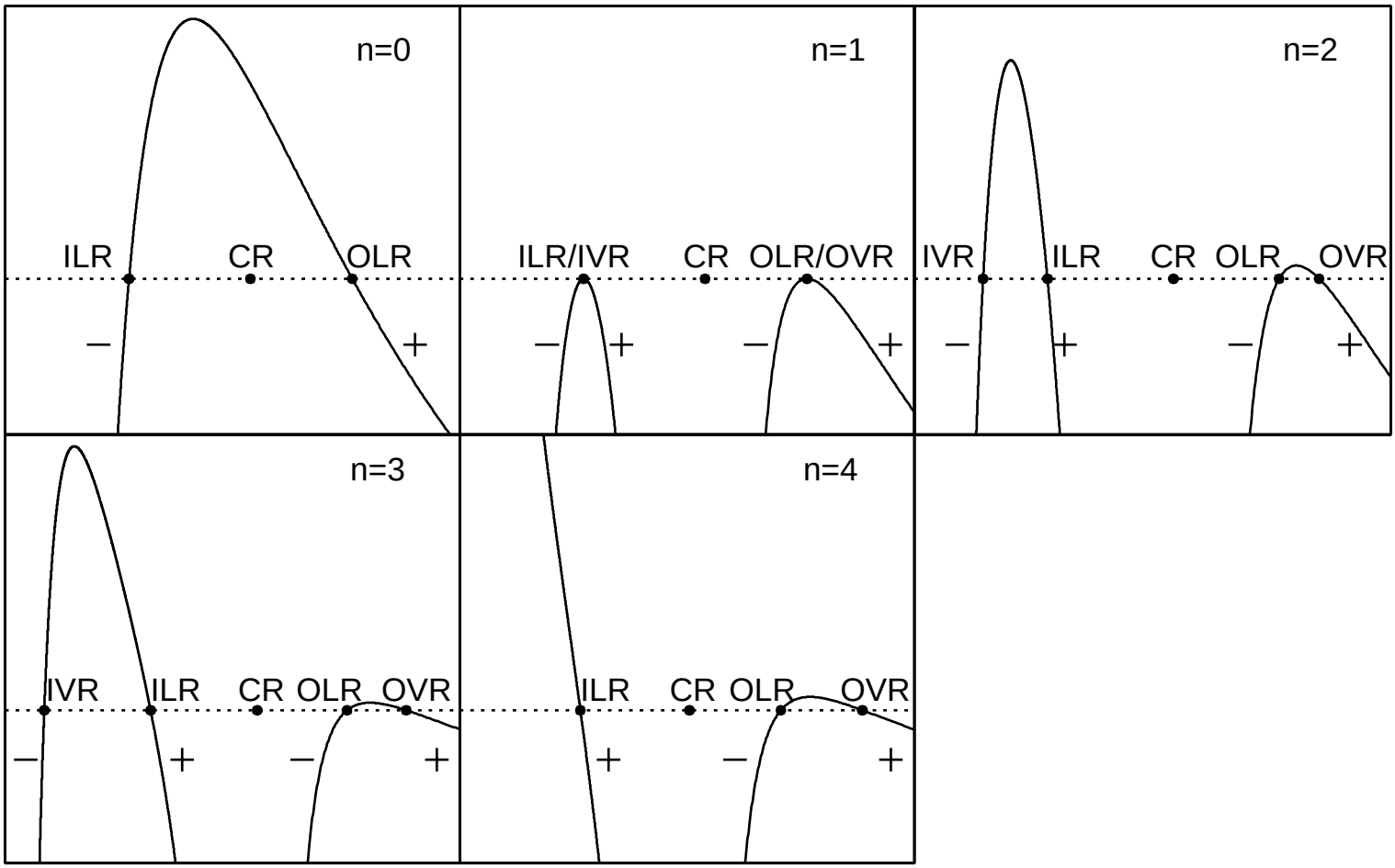

Figure 1. A sketch of the function $G = D(1 - n\Omega_\perp^2/\tilde{\omega}^2)$ as a function of r for $m = 2$ and different values of n (all for $\omega > 0$). The dispersion relation is $G = -k^2c^2$, and thus waves propagate in the regions with $G < 0$. The $\pm$ gives the sign of c_g/c_p of waves in the propagation region.

$$\left(\frac{d^2}{dx^2} - \frac{1}{x}\frac{d}{dx} - \beta x\right)\eta_n = \frac{\psi_n}{x} - \alpha x - \gamma x^2, \tag{42}$$

where ψ_n on the right-hand-side is evaluated at $r = r_L$ and

$$\alpha = \left.\frac{nr^3\phi_n dD/dr}{h^2\tilde{\omega}^2}\right|_{r_L}, \quad \beta = \left.\frac{(\tilde{\omega}^2 - n\Omega_\perp^2)r^3 dD/dr}{h^2\Omega_\perp^2\tilde{\omega}^2}\right|_{r_L},$$
$$\gamma = nr_L^4\left[\frac{\phi_n d^2D/dr^2}{2h^2\tilde{\omega}^2} + \frac{dD}{dr}\frac{d}{dr}\left(\frac{\phi_n}{h^2\tilde{\omega}^2}\right)\right]_{r_L}. \tag{43}$$

Here we have kept the term $-\gamma x^2$ in the Taylor expansion of the second term of right-hand side of Eq.(40) because the leading order term $-\alpha x$ generates only non-wave oscillations, as we shall see later. In orders of magnitudes, $|\beta| \sim (r_L/h)^2$ and $|\alpha| \sim |\gamma| \sim n(r_L/h)^2|\phi_n|$. In particular, for disks with $\Omega_\perp = \kappa = \Omega$ we have

$$\beta = 2(1-n)(1 \pm m)\left(\frac{r^2}{h^2}\frac{d\ln\Omega}{d\ln r}\right)_{r_L}, \tag{44}$$

where upper (lower) sign refers to the OLR (ILR). Note that ILR occurs only for $m \geq 2$, so the factor $(1 \pm m)$ is never zero.

To solve eq. (42), it is convenient to introduce a new variable $\hat{\eta}$ defined by $\eta_n = d\hat{\eta}/dx$ (see Ward 1986). We find

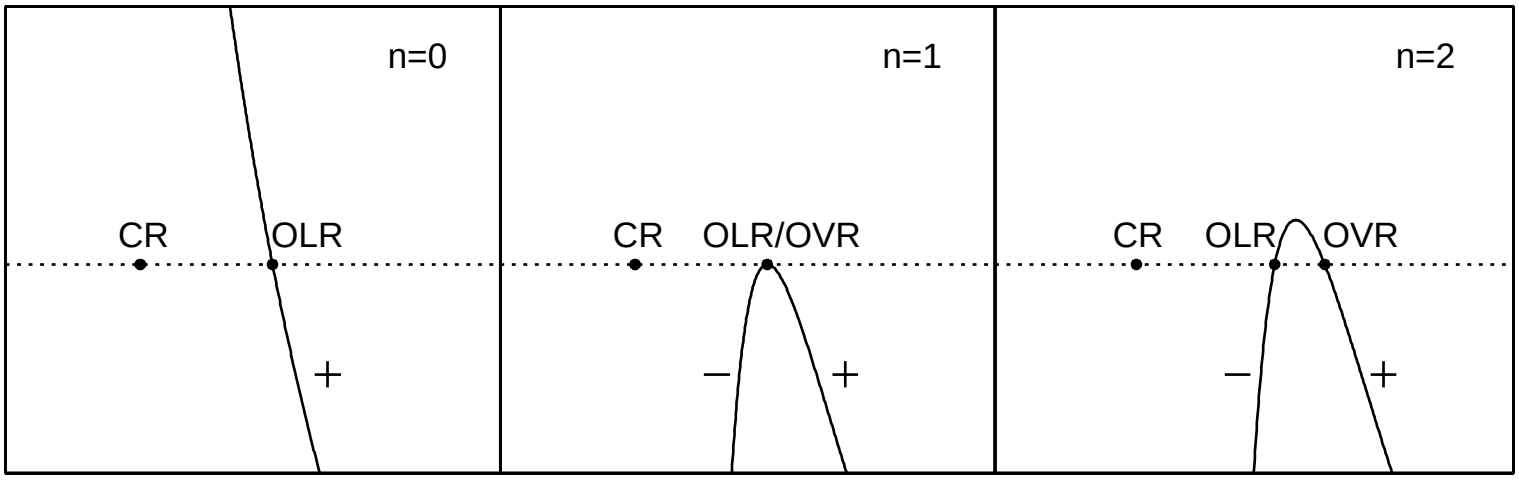

Figure 2. Same as Fig. 1, except for $m = 1$.

$$\frac{d}{dx}\left(\frac{1}{x}\frac{d^2\hat{\eta}}{dx^2}\right) - \beta\frac{d\hat{\eta}}{dx} = \frac{\psi_n}{x^2} - \alpha - \gamma x. \tag{45}$$

Integrating once gives

$$\frac{d^2\hat{\eta}}{dx^2} - \beta x\hat{\eta} = -\psi_n - \alpha x^2 - \frac{1}{2}\gamma x^3 + cx, \tag{46}$$

where c is an integration constant. Then, let

$$y = \hat{\eta} - \frac{\alpha}{\beta}x - \frac{\gamma}{2\beta}x^2 + \frac{c}{\beta}, \tag{47}$$

we have

$$\frac{d^2y}{dx^2} - \beta xy = -\psi_n - \frac{\gamma}{\beta} \equiv \Psi_n. \tag{48}$$

As we see below, introducing the variable y singles out the wave part from η_n. The homogeneous form of Eq.(48) is the Airy equation and its two linearly independent solutions are Airy functions (Abramowiz & Stegun 1964, p. 446):

$$y_1 = Ai(\beta^{1/3}x), \quad y_2 = Bi(\beta^{1/3}x). \tag{49}$$

By the method of variation of parameters, the general solution to the inhomogeneous equation (48) can be written as

$$y = y_2\int_0^x y_1\frac{\Psi_n}{W}dx - y_1\int_0^x y_2\frac{\Psi_n}{W}dx + My_1 + Ny_2, \tag{50}$$

where M and N are constants which should be determined by the boundary conditions, and $W = y_1dy_2/dx - y_2dy_1/dx = \beta^{1/3}/\pi$ is the Wronskian. After writing $\xi = \beta^{1/3}x$, eq. (50) becomes

$$y = \frac{\pi\Psi_n}{\beta^{2/3}}\left[\left(\int_0^\xi Ai(\xi)d\xi + N\right)Bi(\xi) - \left(\int_0^\xi Bi(\xi)d\xi + M\right)Ai(\xi)\right], \tag{51}$$

where we have absorbed a factor $\beta^{2/3}/(\pi\Psi_n)$ into the the constants M and N.

The constants M, N in eq. (51) are determined by boundary conditions at $|\xi| \gg 1$. Note that the condition $|x| = |\beta^{-1/3}\xi| \ll 1$, which is the regime of validity for the solution described in this subsection, implies that $|\xi| \ll |\beta|^{1/3}$. Since $|\beta| \gg 1$, it is reasonable to consider the $|\xi| \gg 1$ asymptotics of eq. (51). In the following we sometimes denote this asymptotics as $|\xi| \to \infty$ for convenience.

For $\xi \gg 1$, the asymptotic expressions of the Airy functions and their integrals are (Abramowiz & Stegun 1964)

$$Ai(\xi) \approx \frac{1}{2}\pi^{-1/2}\xi^{-1/4}e^{-\frac{2}{3}\xi^{3/2}} \to 0, \quad \int_0^\xi Ai(\xi)d\xi \approx \frac{1}{3} - \frac{1}{2}\pi^{-1/2}\xi^{-3/4}e^{-\frac{2}{3}\xi^{3/2}} \to \frac{1}{3},$$

$$Bi(\xi) \approx \pi^{-1/2}\xi^{-1/4}e^{\frac{2}{3}\xi^{3/2}} \to \infty, \quad \int_0^\xi Bi(\xi)d\xi \approx \pi^{-1/2}\xi^{-3/4}e^{\frac{2}{3}\xi^{3/2}} \to \infty. \tag{52}$$

Since $Bi(\xi)$ grows exponentially when $\xi \to \infty$, the coefficient $[\int_0^\xi Ai(\xi)d\xi + N]$ before it in (51) must be very small, otherwise the quantity y (and hence η_n) will become exponentially large, making it impossible to match with any reasonable physical boundary conditions. Without loss of generality, we will take this coefficient to be zero, based on the observation [see eq. (54) below] that the solution on the $\xi < 0$ side is nearly unaffected whether the coefficient is small or precisely zero. Thus $N = -\int_0^\infty Ai(\xi)d\xi = -1/3$. Note that although $\int_0^\xi Bi(\xi)d\xi$ in (51) also exponentially grows when $\xi \to \infty$, it is canceled by $Ai(\xi)$ which is exponentially small. As the Airy functions are monotonic for $\xi > 0$, wave solution does not exist on the side of $\xi > 0$, or

$$(1-n)(1 \pm m)x < 0 \qquad \text{(Nonwave region)} \tag{53}$$

[see eq. (44)]. This is consistent with the wave propagation diagram discussed in §3 (see Figs. 1-2).

Now let us examine the $\xi < 0$ region. For $\xi \ll -1$, the asymptotic behaviors of the Airy functions are

$$\begin{aligned}
&Ai(\xi) \approx \pi^{-1/2}(-\xi)^{-1/4}\sin X(\xi),\\
&\int_0^\xi Ai(\xi)d\xi \approx -\frac{2}{3} + \pi^{-1/2}(-\xi)^{-3/4}\cos X(\xi),\\
&Bi(\xi) \approx \pi^{-1/2}(-\xi)^{-1/4}\cos X(\xi),\\
&\int_0^\xi Bi(\xi)d\xi \approx -\pi^{-1/2}(-\xi)^{-3/4}\sin X(\xi),
\end{aligned} \tag{54}$$

where

$$X(\xi) \equiv \frac{2}{3}(-\xi)^{3/2} + \frac{\pi}{4}. \tag{55}$$

Equation (51) with $N = -1/3$ yields, for $\xi \ll -1$,

$$y \to -\frac{\pi^{1/2}\Psi_n}{2\beta^{2/3}}(-\xi)^{-1/4}\left[(1-iM)e^{iX(\xi)} + (1+iM)e^{-iX(\xi)}\right]. \tag{56}$$

From the relation between η_n and y, we then obtain the asymptotic expression for η_n at $\xi \ll -1$ as

$$\eta_n \to \frac{\alpha}{\beta} + \frac{\gamma}{\beta}x + i\frac{\pi^{1/2}\Psi_n}{2\beta^{1/3}}(-\xi)^{1/4}\left[(1-iM)e^{iX(\xi)} - (1+iM)e^{-iX(\xi)}\right]. \tag{57}$$

The first two terms in eq. (57) describe the non-propagating oscillation, which is called non-wave part by GT. The last term gives traveling waves. Eq. (57) explicitly shows that waves exist on the side of $\xi = \beta^{1/3}x < 0$, or $(1-n)(1 \pm m)x > 0$. Again, this is consistent with the propagation diagram discussed in §3: If $\omega > 0$, the wave zones are located on the outer side of the OLR and inner side of the ILR for $n = 0$, whereas for $n \geq 2$, waves exist on the inner side of the OLR and outer side of the ILR. If $\omega < 0$, LR is possible only for $m = 0$, and the wave zone lies in the outer side of the resonance for $n = 0$ and appears on the inner side for $n \geq 2$.

To determine the constant M, we require that waves excited by the external potential propagate away from the resonance. The direction of propagation of a real wave is specified by its group velocity, as given by eq. (36). For the waves going away from the resonance, we require $\mathrm{sgn}[c_g] = \mathrm{sgn}[x]$, and thus the local wave-number k must satisfy $\mathrm{sgn}[k] = \mathrm{sgn}[x\tilde{\omega}(1-n)]$. On the other hand, the wavenumber associated with the wave term $e^{\pm iX(\xi)}$ in eq. (57) is $k \equiv \pm dX/dr = \mp\beta^{1/3}(-\xi)^{1/2}r_L^{-1}$, which gives $\mathrm{sgn}[k] = \mp\mathrm{sgn}[\beta] = \pm\mathrm{sgn}[x]$ (since $\xi < 0$). Accordingly, if $\omega > 0$, for the $n = 0$ OLR and the $n \geq 2$ ILR, the e^{iX} term represents the outgoing wave, and in order for the e^{-iX} term to vanish, we have $M = i$, which leads to

$$\eta_n \to \bar{\eta} + \tilde{\eta} = \frac{\alpha}{\beta} + \frac{\gamma}{\beta}x + i\frac{\pi^{1/2}\Psi_n}{\beta^{1/3}}(-\xi)^{1/4}e^{iX(\xi)}, \quad (r > r_{_{OLR}} \text{ for } n = 0 \text{ or } r > r_{_{ILR}} \text{ for } n \geq 2) \tag{58}$$

where $\bar{\eta}$ and $\tilde{\eta}$ represent the non-wave part and the wave part, respectively. Similarly, for the $n = 0$ ILR and the $n \geq 2$ OLR, the e^{-iX} term represents the wave propagating away from the resonance, and eliminating the unwanted e^{iX} term requires $M = -i$, which yields

$$\eta_n \to \bar{\eta} + \tilde{\eta} = \frac{\alpha}{\beta} + \frac{\gamma}{\beta}x - i\frac{\pi^{1/2}\Psi_n}{\beta^{1/3}}(-\xi)^{1/4}e^{-iX(\xi)}, \quad (r < r_{_{ILR}} \text{ for } n = 0 \text{ or } r < r_{_{OLR}} \text{ for } n \geq 2). \tag{59}$$

Lindblad resonance also occurs for $\omega < 0$ and $m = 0$, in which case we find that eq. (58) applies for $n \geq 2$ and eq. (59) for $n = 0$.

We can now use eq. (33) to calculate the angular momentum flux carried by the wave excited at the LR. Obviously, the $m = 0$ mode carries no angular momentum. For the $n = 0$ OLR and the $n \geq 2$ ILR, we substitute eq. (58) in eq. (33), and find

$$F_n(r > r_{LR}) = -n!\, m\pi^2 \left(\frac{\sigma\Psi_n^2}{rdD/dr}\right)_{r_L}, \tag{60}$$

where, according to eqs. (39), (43) and (48),

$$\Psi_n = \left\{ -r\frac{d\phi_n}{dr} + \frac{2m\Omega}{\omega - m\Omega}\phi_n + n\left[\mu - \frac{\Omega_\perp^2 r}{2(\kappa^2 - n\Omega_\perp^2)}\frac{d}{dr}\ln\left(\frac{\phi_n^2}{h^4\kappa^4}\frac{dD}{dr}\right)\right]\phi_n \right.$$
$$\left. +(n+1)(n+2)\mu\,\phi_{n+2} \right\}_{r_L}. \tag{61}$$

Similarly, for $n = 0$ ILR and $n \geq 2$ OLR, we use eq. (59) in eq. (33) to find

$$F_n(r < r_{LR}) = n!\, m\pi^2 \left(\frac{\sigma\Psi_n^2}{rdD/dr}\right)_{r_L}. \tag{62}$$

Obviously, the angular momentum flux at the $\xi > 0$ side (where no wave can propagate) vanishes. Note that the torque on the disk through waves excited in $r > r_{LR}$ is $F_n(r > r_{LR})$, while for waves excited in $r < r_{LR}$ the torque is $-F_n(r < r_{LR})$. Since $dD/dr < 0$ for OLR and > 0 for ILR, we find that for both $n = 0$ and $n \geq 2$, the total torque on the disk through both IRL and OLR is

$$T_n(\text{OLR and ILR}) = |F_{ORL}| - |F_{ILR}| = -n!\, m\pi^2 \left[\left(\frac{\sigma\Psi_n^2}{rdD/dr}\right)_{\rm OLR} + \left(\frac{\sigma\Psi_n^2}{rdD/dr}\right)_{\rm ILR}\right]. \tag{63}$$

That is, independent of n, the torque on the disk is always positive at OLR and negative at ILR (see GT). We note that for $n = \mu = 0$, our result agrees with that for the 2D non-self-gravitating disks (GT; Ward 1986).

4.2 $n = 1$ Mode: Lindblad/Vertical Resonances

For $n = 1$, the LR and VR are degenerate for a Keplerian disk, and we shall call them Linblad/vertical resonances (L/VRs) ‖. The resonance radius $r = r_L$ is both a (apparent) singular point and a second-order turning point of the wave equation (40). The wave propagation diagram (see Fig. 1-2) shows that waves exist on both sides of a L/VR.

Expanding eq. (40) in the vicinity of the resonance ($|x| \ll 1$), we have

$$\frac{d^2}{dx^2}\eta_1 - \frac{1}{x}\frac{d}{dx}\eta_1 + b^2x^2\eta_1 = \frac{\psi_1}{x} - \alpha_1 x, \tag{64}$$

where

$$\alpha_1 = \left.\frac{r^3\phi_1 dD/dr}{h^2\tilde{\omega}^2}\right|_{r_L}, \quad b = \left|\frac{r^2 dD/dr}{h\Omega_\perp^2}\right|_{r_L}, \quad \psi_1 = \left[\left(r\frac{d}{dr} - \frac{2m\Omega}{\tilde{\omega}} - \mu\right)\phi_1 - 6\mu\phi_3\right]_{r_L}. \tag{65}$$

In orders of magnitudes, $|\alpha_1| \sim (r_L/h)^2\phi_1$ and $b \sim r_L/h$. Substitution of $\eta_1 = y - \psi_1 x$ into eq. (64) gives

$$\frac{d^2}{dx^2}y - \frac{1}{x}\frac{d}{dx}y + b^2x^2y = b^2\psi_1 x^3 - \alpha_1 x. \tag{66}$$

The two linearly independent solutions to the corresponding homogeneous form of eq. (66) are

$$y_1 = e^{-ibx^2/2}, \quad y_2 = e^{ibx^2/2}. \tag{67}$$

The method of variation of parameters then gives the general solution of eq. (66):

$$y = e^{i\zeta^2/2}\left[\int_{-\infty}^{\zeta} e^{-i\zeta^2/2}S(\zeta)d\zeta + N\right] + e^{-i\zeta^2/2}\left[\int_{\zeta}^{\infty} e^{i\zeta^2/2}S(\zeta)d\zeta + M\right], \tag{68}$$

where we have defined $\zeta = b^{1/2}x$ and

$$S(\zeta) = \frac{\psi_1\zeta^2}{2ib^{1/2}} - \frac{\alpha_1}{2ib^{3/2}}. \tag{69}$$

Note that although our analysis is limited to $|x| \ll 1$, we have extended the integration limit to $\zeta = \pm\infty$ in eq. (68) — This is valid because $b \sim r_L/h \gg 1$ for a thin disk and the integrands in the integrals are highly oscillatory for $|\zeta| \gg 1$ (so that the

‖ Bate et al. (2002) previously analysed the mixed L/VRs for axisymmetric waves ($m = 0$); such waves do not carry angular momentum.

contribution to the integrals from the $|\zeta| \gg 1$ region is negligible; see Wong 2001). The wave solution in the $|\zeta| \gg 1$ region is approximately given by

$$y = \left[\int_{-\infty}^{\infty} e^{-i\zeta^2/2} S(\zeta) d\zeta + N\right] e^{i\zeta^2/2} + M e^{-i\zeta^2/2}, \qquad (\zeta \gg 1) \tag{70}$$

$$y = \left[\int_{-\infty}^{\infty} e^{i\zeta^2/2} S(\zeta) d\zeta + M\right] e^{-i\zeta^2/2} + N e^{i\zeta^2/2}, \qquad (\zeta \ll -1). \tag{71}$$

The constants M and N can be fixed by requiring that no waves propagate into the resonance. From our analysis of the wave group velocity in §3 (see Figs. 1-2), we find that for the waves propagating away from the resonance, the local wavenumber must be positive, irrespective of whether it is inner or outer $n = 1$ L/VR. Accordingly, we must have $M = 0$ [from eq. (70)] and $N = 0$ [from eq. (71)]. Since the integral

$$\int_{-\infty}^{\infty} e^{\pm i\zeta^2/2} S(\eta) d\zeta = \sqrt{\frac{\pi}{2}} \left(\pm \frac{\psi_1}{b^{1/2}} + i \frac{\alpha_1}{b^{3/2}}\right) e^{\pm i\pi/4}. \tag{72}$$

eqs. (70)-(71) reduce to

$$y \simeq \sqrt{\frac{\pi}{2}} \left(-\frac{\psi_1}{b^{1/2}} + i \frac{\alpha_1}{b^{3/2}}\right) e^{i\frac{1}{2}\zeta^2 - i\frac{\pi}{4}}, \qquad (\zeta \gg 1), \tag{73}$$

$$y \simeq \sqrt{\frac{\pi}{2}} \left(\frac{\psi_1}{b^{1/2}} + i \frac{\alpha_1}{b^{3/2}}\right) e^{-i\frac{1}{2}\zeta^2 + i\frac{\pi}{4}}, \qquad (\zeta \ll -1). \tag{74}$$

Using eqs. (33) and (73), we find that the angular momentum flux carried outward from the resonance (toward larger radii) by the wave excited at a L/VR is given by

$$F_1(r > r_{_{L/VR}}) = -\frac{m\pi^2 \sigma_L}{2 r_L (dD/dr)_L} \left(\psi_1^2 + \alpha_1^2/b^2\right) \simeq -\frac{m\pi^2}{2} \left(\frac{r\sigma\phi_1^2}{h^2 dD/dr}\right)_{r_L}, \tag{75}$$

where in the second equality we have used the fact $|\alpha_1/b| = (r/h)|\phi_1| \gg |\psi_1|$. Similarly, using (74), we find that the angular momentum flux carried by the $x < 0$ wave is

$$F_1(r < r_{_{L/VR}}) = \frac{m\pi^2}{2} \left(\frac{r\sigma\phi_1^2}{h^2 dD/dr}\right)_{r_L}. \tag{76}$$

Thus the angular momentum transfer to the disk through a L/VR is simply $T_1(\text{L/VR}) = F_1(r > r_{_{L/VR}}) - F_1(r < r_{_{L/VR}}) = 2F_1(r > r_{_{L/VR}})$. Combining the inner and outer resonances, the total torque is

$$T_1(\text{OL/VR and IL/VR}) = -m\pi^2 \left[\left(\frac{r\sigma\phi_1^2}{h^2 dD/dr}\right)_{\text{OL/VR}} + \left(\frac{r\sigma\phi_1^2}{h^2 dD/dr}\right)_{\text{IL/VR}}\right]. \tag{77}$$

Again, we find that the torque on the disk is positive at OL/VR and negative at IL/VR. Comparing the above result with the results of §4.1 and §5, we find that although the $n = 1$ L/VR involves a combination of LR and VR its behavior is more like a VR.

5 VERTICAL RESONANCES ($N \geq 2$)

We have already studied the $n = 1$ vertical resonance in §4.2. We now examine VRs, $\tilde{\omega}^2 = n\Omega_\perp^2$, for $n \geq 2$.

In the neighborhood of a VR, there is no singularity in eq. (29). For a thin disk ($h \ll r$) with $m, n \ll (r/h)$, it is only necessary to keep $d^2\eta_n/dr^2$ and the terms that are $\propto c^{-2} \propto h^{-2}$. This can be justified rigorously from the asymptotic theory of differential equations (e.g., Olver 1974), which shows that the discarded terms have no contribution to the leading order of the asymptotic solution. Indeed, the discarded terms only make a small shift to the vertical resonance for a thin disk. As for the coupling terms with other modes, in addition to the reasons given in §4, the dropping of the coupling terms are more strongly justified here as the VRs with different n's are located at different radii and their mutual effects can be considered insignificant. Therefore, around the VR radius $r_{_V}$, we can simplify eq. (29) to

$$\frac{d^2}{dr^2}\eta_n - \frac{D(\tilde{\omega}^2 - n\Omega_\perp^2)}{h^2\tilde{\omega}^2\Omega_\perp^2}\eta_n = -\frac{nD}{h^2\tilde{\omega}^2}\phi_n. \tag{78}$$

Changing the variable from r to $x = (r - r_{_V})/r_{_V}$, we obtain, for $|x| \ll 1$,

$$\frac{d^2}{dx^2}\eta_n - \lambda x \eta_n = \chi, \tag{79}$$

where

$$\lambda = -\frac{2r^3 D(m\tilde{\omega} d\Omega/dr + n\Omega_\perp d\Omega_\perp/dr)}{h^2\tilde{\omega}^2\Omega_\perp^2}\bigg|_{r_V}, \quad \chi = -\frac{nr^2 D\phi_n}{h^2\tilde{\omega}^2}\bigg|_{r_V}. \tag{80}$$

Similar to §4.1, the general solution to eq. (79) reads

$$\eta_n = \frac{\pi\chi}{\lambda^{2/3}}\left[\left(\int_0^\varsigma Ai(\varsigma)d\varsigma + N\right)Bi(\varsigma) - \left(\int_0^\varsigma Bi(\varsigma)d\varsigma + M\right)Ai(\varsigma)\right], \tag{81}$$

where $\varsigma = \lambda^{\frac{1}{3}}x$. Suppressing the mode which is exponentially large when $\varsigma \to \infty$ yields $N = -1/3$.

Waves can propagate in the $\varsigma < 0$ region, i.e., on the outer side of the OVR and on the inner side of the IVR (see Figs. 1-2). For the waves to propagate away from the resonance, we require the group velocity to satisfy $\mathrm{sgn}[c_g] = \mathrm{sgn}[x]$, and hence the local wavenumber to satisfy $\mathrm{sgn}[k] = \mathrm{sgn}[x\tilde{\omega}(1-n^{-1})]$. Thus, if $\omega > 0$, we demand that as $\varsigma \to -\infty$, $\eta_n \propto e^{i\frac{2}{3}(-\varsigma)^{3/2}}$ for the OVR and $\eta_n \propto e^{-i\frac{2}{3}(-\varsigma)^{3/2}}$ for the IVR. This determines M and yields, for $\varsigma \to -\infty$,

$$\eta_n \to -\frac{\pi^{1/2}\chi}{\lambda^{2/3}}(-\varsigma)^{-\frac{1}{4}}\exp\left[i(\frac{2}{3}(-\varsigma)^{3/2} + \frac{\pi}{4})\right], \qquad (r > r_{OVR}) \tag{82}$$

$$\eta_n \to -\frac{\pi^{1/2}\chi}{\lambda^{2/3}}(-\varsigma)^{-\frac{1}{4}}\exp\left[-i(\frac{2}{3}(-\varsigma)^{3/2} + \frac{\pi}{4})\right], \qquad (r < r_{IVR}). \tag{83}$$

The angular momentum flux is then

$$F_n(r > r_{OVR}) = n!\, m\pi^2\left(\frac{\sigma\chi^2}{\lambda D}\right)_{r_V} = -\frac{\pi^2}{2}n!\sqrt{n}\frac{m}{\sqrt{n}+m}\left(\frac{r\sigma\phi_n^2}{h^2\Omega d\Omega/dr}\right)_{\rm OVR}, \tag{84}$$

$$F_n(r < r_{IVR}) = -n!\, m\pi^2\left(\frac{\sigma\chi^2}{\lambda D}\right)_{r_V} = \frac{\pi^2}{2}n!\sqrt{n}\frac{m}{\sqrt{n}-m}\left(\frac{r\sigma\phi_n^2}{h^2\Omega d\Omega/dr}\right)_{\rm IVR}. \tag{85}$$

The torque on the disk is $F_n(r > r_{OVR})$ at OVR and $-F_n(r < r_{IVR})$ at IVR. Note that the IVR exists only for $m > \sqrt{n}$ (see §3), so $-F_n(r < r_{IVR}) < 0$. The total torque on the disk due to both OVR and IVR is

$$T_n(\text{OVR and IVR}) = -\frac{\pi^2}{2}n!\sqrt{n}\left[\frac{m}{\sqrt{n}+m}\left(\frac{r\sigma\phi_n^2}{h^2\Omega d\Omega/dr}\right)_{\rm OVR} + \frac{m}{\sqrt{n}-m}\left(\frac{r\sigma\phi_n^2}{h^2\Omega d\Omega/dr}\right)_{\rm IVR}\right]. \tag{86}$$

(Obviously, in the above expression, the IVR contribution should be set to zero if $m < \sqrt{n}$). Again, we see that the torque is positive at OVR and negative at IVR.

If $\omega < 0$, a single VR exists for $m < \sqrt{n}$. In this case waves are generated on the outer side of the resonance with

$$\eta_n(r > r_V) \to -\frac{\pi^{1/2}\chi}{\lambda^{2/3}}(-\varsigma)^{-\frac{1}{4}}\exp\left[-i(\frac{2}{3}(-\varsigma)^{3/2} + \frac{\pi}{4})\right], \qquad (r > r_V;\ \text{ for } \omega < 0) \tag{87}$$

as $\varsigma = \lambda^{1/3}x \to -\infty$. Thus

$$F_n(r > r_V) = \frac{\pi^2}{2}n!\sqrt{n}\frac{m}{\sqrt{n}-m}\left(\frac{r\sigma\phi_n^2}{h^2\Omega d\Omega/dr}\right)_{r_V}, \qquad (\omega < 0). \tag{88}$$

The torque on the disk due to such VR is negative.

It is interesting to compare our result with the one derived from shearing sheet model (Takeuchi & Miyama 1998; Tanaka et al 2002):

$$F_n = \frac{\pi^2}{2}n!\sqrt{n}\left(\frac{r\sigma\phi_n^2}{h^2\Omega|d\Omega/dr|}\right)_{r_V}. \tag{89}$$

Clearly, our eq. (84) reduces to eq. (89) for $m \gg \sqrt{n}$.

At this point, it is useful to compare the amplitudes of the waves generated at different resonances. For LRs, $F_n \sim \sigma\phi_n^2/\Omega^2$; for both the $n = 1$ L/VRs and $n \geq 2$ VRs, $F_n \sim (r/h)^2\sigma\phi_n^2/\Omega^2$. Thus, when the external potential components have the same orders of magnitude, the angular momentum transfer through VRs is larger than LRs for thin disks. Since we expect $\phi_n \propto (h/r)^n$, the $n = 1$ vertical resonance may be comparable to the $n = 0$ Lindblad resonace in transferring angular momentum.

6 COROTATION RESONANCES

Corotation resonances (CRs), where $\tilde{\omega} = 0$ or $\omega = m\Omega$, may exist in disks for $\omega > 0$. The WKB dispersion relation and wave propagation diagram discussed in §3 (see Fig. 1-2) show that for $n = 0$, waves are evanescent in the region around the

corotation radius r_c, while for $n > 0$ wave propagation is possible around r_c. This qualitative difference is also reflected in the behavior of the singularity in eq. (29). We treat the $n = 0$ and $n > 0$ cases separately.

6.1 $n = 0$ Mode

In the vicinity of corotation, we only need to keep the terms in eq. (29) that contain the $\tilde{\omega}^{-1}$ singularity and the term $\propto h^{-2}$. The term $\propto \eta_{n+2}/\tilde{\omega}$ can also be dropped, since from eq. (26) we can see that the coupling term is negligible when $|\tilde{\omega}|$ is small. Thus for $n = 0$, eq. (29) can be approximately simplified to

$$\frac{d^2}{dr^2}\eta_0 - \frac{2m\Omega}{r\tilde{\omega}}\left(\frac{d}{dr}\ln\frac{\sigma\Omega}{D}\right)\eta_0 - \frac{D}{h^2\Omega_\perp^2}\eta_0 = \frac{2m\Omega}{r\tilde{\omega}}\left(\frac{d}{dr}\ln\frac{\sigma\Omega}{D}\right)\phi_0 + \frac{4\mu m\Omega}{r^2\tilde{\omega}}\phi_2. \tag{90}$$

Near the corotation radius r_c, we introduce the variable $x = (r - r_c)/r_c$, and eq. (90) becomes

$$\frac{d^2\eta_0}{dx^2} + \left(\frac{p}{x+i\epsilon} - q^2\right)\eta_0 = -\frac{p}{x+i\epsilon}\Phi, \tag{91}$$

where

$$p = \left[\frac{2\Omega}{d\Omega/dr}\frac{d}{dr}\ln\left(\frac{\sigma\Omega}{D}\right)\right]_{r_c}, \quad q = \left|\frac{Dr^2}{h^2\Omega_\perp^2}\right|^{1/2}_{r_c} = (\kappa r/c)_{r_c} \gg 1, \tag{92}$$

$$\Phi = \left[\phi_0 + \frac{2\mu\phi_2}{rd\ln(\sigma\Omega/D)/dr}\right]_{r_c}. \tag{93}$$

In eq. (91), the small imaginary part $i\epsilon$ (with $\epsilon > 0$) in $1/x$ arises because we consider the response of the disk to a slowly increasing perturbation (GT) or because a real disk always has some dissipation which has not been explicitly included in our analysis. If $\mu = 0$ or $|\phi_2| \ll |\phi_0|$, then the eq. (91) is the same as the equation studied by GT for 2D disks.

Goldreich & Tremaine (1979) solved eq. (91) neglecting the $(p/x)\eta_0$ term, and found that there is a net flux of angular momentum into the resonance, given by

$$\Delta F_c = F(r_c-) - F(r_c+) = 2\pi^2 m\left[\frac{\Phi^2}{d\Omega/dr}\frac{d}{dr}\left(\frac{\sigma\Omega}{D}\right)\right]_{r_c}. \tag{94}$$

On the other hand, integrating eq. (91) from $x = 0-$ to $x = 0+$ gives $(d\eta_0/dx)_{0+} - (d\eta_0/dx)_{0-} = i\pi p(\eta_0 + \Phi)$, which, together with eq. (32), yield (Tanaka et al. 2002)

$$\Delta F_c = 2\pi^2 m\left[\frac{|\eta_0 + \Phi|^2}{d\Omega/dr}\frac{d}{dr}\left(\frac{\sigma\Omega}{D}\right)\right]_{r_c}. \tag{95}$$

Tanaka et al. (2002) argued that neglecting η_0 in eq. (95) may be not justified in a gaseous disk and that the revised formula (95) fits their numerical result better than eq. (94).

Although eq. (95) is a precise result of eq. (91), the presence of the unknown quantity $\eta_0(r_c)$ makes the expression not directly useful. Therefore, a more rigorous solution of eq. (91) without dropping the $(p/x)\eta_0$ term seems desirable. In the following we provide such a solution.

After changing variable $w \equiv \eta_0 + \Phi$, eq. (91) becomes

$$\frac{d^2w}{dx^2} + (\frac{p}{x} - q^2)w = -q^2\Phi. \tag{96}$$

To solve this non-homogeneous equation, we need firstly to find the solutions of the corresponding homogeneous equation

$$\frac{d^2w}{dx^2} + (\frac{p}{x} - q^2)w = 0. \tag{97}$$

By introducing the variables

$$w = xe^{qx}y, \quad s = -2qx, \tag{98}$$

eq. (97) is transformed to Kummer's equation (Abramowitz & Stegun 1964)

$$s\frac{d^2y}{ds^2} + (2-s)\frac{dy}{ds} - (1 + \frac{p}{2q})y = 0. \tag{99}$$

Its two independent solutions can be chosen as

$$y_1 = U(1 + \frac{p}{2q}, 2, s), \quad y_2 = e^s U(1 - \frac{p}{2q}, 2, -s), \tag{100}$$

where the function U is a logarithmic solution defined as

$$U(a,n+1,z) = \frac{(-1)^{n+1}}{n!\Gamma(a-n)}\Bigg[M(a,n+1,z)\ln z + \sum_{r=0}^{\infty}\frac{(a)_r z^r}{(n+1)_r r!}\{\psi(a+r)-\psi(1+r)-\psi(1+n+r)\}\Bigg] + \frac{(n-1)!}{\Gamma(a)}z^{-n}\sum_{r=0}^{n-1}\frac{(a-n)_r z^r}{(1-n)_r r!}, \tag{101}$$

in which $M(a,b,z)$ is Kummer's function, ψ is the Digamma function and $(...)_r$ denotes the Pochhammer symbol (see Abramowitz & Stegun 1964). So the two independent solutions to eq. (97) are

$$w_1 = xe^{qx}U(1+\frac{p}{2q},2,-2qx), \quad w_2 = xe^{-qx}U(1-\frac{p}{2q},2,2qx), \tag{102}$$

and their Wronskian can be shown to be

$$W = w_1\frac{d}{dx}w_2 - w_2\frac{d}{dx}w_1 = -\frac{1}{2q}e^{i\pi(1-\frac{p}{2q})}. \tag{103}$$

Note that owing to the singularity of the function U at the branch point $x=0$, a branch cut has been chosen in the lower half of the complex plane.

The solution to eq. (96) has the form

$$\begin{aligned} w &= w_2\int_{-\infty}^{x} w_1\frac{-q^2\Phi}{W}dx + w_1\int_{x}^{\infty} w_2\frac{-q^2\Phi}{W}dx \\ &= 2q^3\Phi e^{-i\pi(1-\frac{p}{2q})}xe^{-qx}U(1-\frac{p}{2q},2,2qx)\int_{-\infty}^{x} xe^{qx}U(1+\frac{p}{2q},2,-2qx)dx \\ &\quad +2q^3\Phi e^{-i\pi(1-\frac{p}{2q})}xe^{qx}U(1+\frac{p}{2q},2,-2qx)\int_{x}^{\infty} xe^{-qx}U(1-\frac{p}{2q},2,2qx)dx, \end{aligned} \tag{104}$$

where we have adopted the physical boundary conditions that for $|qx|\gg 1$, the quantity $|w|$ does not become exponentially large. One of the limits of each integration has been extend to infinity since it only introduces negligible error due to the property of the integrand. From eq. (101), at $x=0$, we have

$$w(x=0) = -\frac{\Phi}{4}e^{-i\pi(1-\frac{p}{2q})}\frac{1}{\Gamma(1-\frac{p}{2q})}\int_0^{\infty} e^{-\frac{1}{2}t}tU(1+\frac{p}{2q},2,t)dt - \frac{\Phi}{4}e^{-i\pi(1-\frac{p}{2q})}\frac{1}{\Gamma(1+\frac{p}{2q})}\int_0^{\infty} e^{-\frac{1}{2}t}tU(1-\frac{p}{2q},2,t)dt \ . \tag{105}$$

Utilizing a formula of Laplace transform (Erdélyi et al. 1953)

$$\int_0^{\infty} e^{-st}t^{b-1}U(a,c,t)dt = \frac{\Gamma(b)\Gamma(b-c+1)}{\Gamma(a+b-c+1)}\ {}_2F_1(b,b-c+1;a+b-c+1;1-s) \tag{106}$$

to calculate out the integrals, we obtain

$$w(x=0) = -\frac{\Phi}{4}e^{-i\pi(1-\frac{p}{2q})}\frac{\sin\frac{p\pi}{2q}}{\frac{p}{2q}\pi}\left[\frac{{}_2F_1(2,1;2+\frac{p}{2q};\frac{1}{2})}{1+\frac{p}{2q}} + \frac{{}_2F_1(2,1;2-\frac{p}{2q};\frac{1}{2})}{1-\frac{p}{2q}}\right], \tag{107}$$

where ${}_2F_1$ denotes the Gaussian hypergeometric function. Hence,

$$\eta_0(r_c) = \frac{1}{4}e^{i\frac{p\pi}{2q}}\frac{\sin\frac{p\pi}{2q}}{\frac{p}{2q}\pi}\left[\frac{{}_2F_1(2,1;2+\frac{p}{2q};\frac{1}{2})}{1+\frac{p}{2q}} + \frac{{}_2F_1(2,1;2-\frac{p}{2q};\frac{1}{2})}{1-\frac{p}{2q}}\right]\Phi - \Phi, \tag{108}$$

and from eq. (95),

$$\Delta F_c = 2\pi^2 m\left[\frac{\Phi^2}{d\Omega/dr}\frac{d}{dr}\left(\frac{\sigma\Omega}{D}\right)\right]_{r_c} \times\frac{1}{16}\frac{\sin^2\frac{p\pi}{2q}}{\left(\frac{p}{2q}\pi\right)^2}\left[\frac{{}_2F_1(2,1;2+\frac{p}{2q};\frac{1}{2})}{1+\frac{p}{2q}} + \frac{{}_2F_1(2,1;2-\frac{p}{2q};\frac{1}{2})}{1-\frac{p}{2q}}\right]^2. \tag{109}$$

By the fact ${}_2F_1(2,1;2;\frac{1}{2}) = 2$, it is easy to check that when $p/q\sim h/r\to 0$, $|\eta_0(r_c)|$ becomes much smaller than $|\Phi|$, and ΔF_c reduces to eq. (94), the original Goldreich-Tremaine result.

6.2 $n \geq 1$ Mode

In the vicinity of corotation with $n \geq 1$, the terms $\propto h^{-2}$ in eq. (29) are dominant, and we only need to keep these terms and the second-order differential term. Eq. (29) reduces to

$$\frac{d^2}{dr^2}\eta_n - \frac{D(\tilde{\omega}^2 - n\Omega_\perp^2)}{h^2\tilde{\omega}^2\Omega_\perp^2}\eta_n = -\frac{nD}{h^2\tilde{\omega}^2}\phi_n, \tag{110}$$

where ϕ_n is evaluated at $r = r_c$. Defining $x = (r - r_c)/r_c$ and expanding eq. (110) around $x = 0$, we have

$$\frac{d^2\eta_n}{dx^2} + C\frac{1}{(x + i\epsilon)^2}\eta_n = -C\frac{\phi_n}{(x + i\epsilon)^2} \tag{111}$$

where

$$C = \frac{n}{m^2}\left(\frac{\kappa}{h\, d\Omega/dr}\right)^2_{r_c} \sim \frac{n}{m^2}\left(\frac{r_c}{h}\right)^2 \gg 1. \tag{112}$$

We remark here that eq. (110) is similar to the equation derived in the context of the stability analysis of stratified flows (Booker & Bretherton 1967), although the physics here is quite different.

The general solution to eq. (111) is

$$\eta_n = -\phi_n + Mz^{1/2}z^{i\nu} + Nz^{1/2}z^{-i\nu} = -\phi_n + Mz^{1/2}e^{i\nu\ln z} + Nz^{1/2}e^{-i\nu\ln z}, \tag{113}$$

where $\nu = \sqrt{C - \frac{1}{4}} \gg 1$, $z = x + i\epsilon$ (with $\epsilon > 0$) and M and N are constants. The first term, the non-wave part, is a particular solution, while the other two terms are solutions to the homogeneous equation, depicting the waves.

From eq. (36), we find that the group velocity of a wave (with wave number k) near corotation is given by $c_g = -c\tilde{\omega}^2/(\sqrt{n}\kappa\Omega_\perp)\mathrm{sgn}(k\tilde{\omega})$. Thus $\mathrm{sgn}(c_g) = -\mathrm{sgn}(kx)$ for $|x| > 0$. The $z^{1/2}z^{i\nu}$ component in eq. (113) has local wave number $k = d(\nu\ln z)/dr = \nu/(r_c x)$, and thus it has group velocity $c_g < 0$. If we require no wave to propagate into $x = 0$ from the $x > 0$ region (as we did in studying LRs and VRs; see §4 and §5), then we must have $M = 0$. Similarly, requiring no wave to propagate into corotation from the $x < 0$ region gives $N = 0$. Thus we have shown explicitly that waves are not excited at corotation. Further calculation shows that even adding the higher-order terms to eq. (111) does not alter this conclusion. This is understandable because $|k| \to \infty$ near corotation, and short-wavelength perturbations couple weakly to the external potential.

However, unlike the $n = 0$ case, waves with $n \geq 1$ can propagate into the corotation region and get absorbed at the corotation. To calculate this absorption explicitly, let us consider an incident wave propagating from the $x > 0$ region toward $x = 0$:

$$\eta_n = A_+\, x^{1/2}e^{i\nu\ln x}, \qquad (x > 0;\ \text{ incident wave}), \tag{114}$$

where A_+ is constant specifying the wave amplitude. To determine the transmitted wave, we note that $z = 0$ is the branch point of the function $e^{i\nu\ln z}$, and the physics demands that the solution to eq. (111) be analytic in the complex plane above the real axis. Thus we must decide the branch cut of the function so that it is single-valued. As discussed before (see §6.1), while our analysis in this paper does not explicitly include dissipation, a real disk certainly will have some viscosity, and viscous effect can be mimicked in our analysis by adding a small imaginary part $i\epsilon$ (with $\epsilon > 0$) to the frequency ω. Alternatively, this can be understood from causality where the disturbing potential is assumed to be turned on slowly in the distant past. This is the origin of imaginary part of $z = x + i\epsilon$ in eq. (111) or eq. (113). Therefore, we can choose the negative imaginary axis as the branch cut of the function $e^{i\nu\ln z}$. In doing so, we have $e^{i\nu\ln z} = e^{i\nu(\ln|x| + i\pi)}$ for $x < 0$. Thus the transmitted wave is given by

$$\eta_n = i\, A_+\, e^{-\pi\nu}(-x)^{1/2}e^{i\nu\ln(-x)}, \qquad (x < 0;\ \text{ transmitted wave}). \tag{115}$$

Since $\nu \gg 1$, the wave amplitude is vastly decreased by a factor $e^{-\pi\nu}$ after propagating through the corotation. From eq. (32) or (33), the net angular momentum flux absorbed at corotation is

$$\begin{aligned}\Delta F_c &= F_n(r_c-) - F_n(r_c+) = n!\,\pi m\left(\frac{\sigma}{\kappa^2}\right)_{r_c}\nu|A_+|^2(1 + e^{-2\pi\nu}) \\ &\simeq n!\,\sqrt{n}\pi\left(\frac{\sigma}{\kappa h|d\Omega/dr|}\right)_{r_c}|A_+|^2,\end{aligned} \tag{116}$$

where in the last equality we have used $\nu \simeq \sqrt{C} \gg 1$.

Similarly, consider a wave propagating from $x < 0$ toward $x = 0$:

$$\eta_n = A_- z^{1/2}e^{-i\nu\ln z} = iA_- e^{\pi\nu}(-x)^{1/2}e^{-i\nu\ln(-x)}, \qquad (x < 0;\ \text{ incident wave}). \tag{117}$$

The transmitted wave is simply

$$\eta_n = A_- x^{1/2} e^{-i\nu \ln x}, \qquad (x > 0; \quad \text{transmitted wave}). \tag{118}$$

The net angular momentum flux into the corotation is

$$\Delta F_c = -n!\,\pi m \left(\frac{\sigma}{\kappa^2}\right)_{r_c} \nu |A_- e^{\pi\nu}|^2 (1 + e^{-2\pi\nu}) \simeq -n!\,\sqrt{n}\pi \left(\frac{\sigma}{\kappa h |d\Omega/dr|}\right)_{r_c} |A_- e^{\pi\nu}|^2, \tag{119}$$

where the negative value of ΔF_c arises because waves inside corotation carry negative angular momentum.

In summary, for $n \geq 1$, waves propagating across the corotation are attenuated (in amplitude) by a factor $e^{-\pi\nu}$. Thus the corotation can be considered as a sink for waves with $n \geq 1$ — a similar conclusion was reached by Kato (2003) and Li et al. (2003), who were concerned with the stability of oscillation modes in accretion disks around black hole. The parameters A_+, A_- in eqs. (114) and (117) are determined by boundary conditions. In Appendix B, we discuss a specific example where waves excited at Lindblad/vertical resonances propagate into the corotation and get absorbed and transfer their angular momenta there.

7 WAVE EXCITATIONS AT DISK BOUNDARIES

In the preceding sections we have examined the effects of various resonances in a disk. Even without any resonance, density/bending waves may be excited at disk boundaries.

To give a specific example, let us consider the $n = m = 1$ bending wave in a Keplerian disk driven by a potential with frequency ω in the range $0 < \omega < \Omega(r_{out})$. Here we use r_{out} and r_{in} to denote the outer and inner radii of the disk. This situation occurs, for example, when we consider perturbations of the circumstellar disk of the primary star driven by the secondary in a binary system. Since no resonance condition is satisfied for the whole disk, the general solution to the disk perturbation is given by [see eq. (A9) in Appendix A]**

$$\eta_1 = Q^{-1}G + (D/r\sigma)^{1/2} Q^{-1/4} \left[M \exp(-i \int_{r_{in}}^{r} Q^{1/2} dr) + N \exp(i \int_{r_{in}}^{r} Q^{1/2} dr) \right], \tag{120}$$

where

$$Q = k^2 = \frac{D(\Omega_\perp^2 - \tilde{\omega}^2)}{h^2 \tilde{\omega}^2 \Omega_\perp^2}, \qquad G = -\frac{D}{h^2\tilde{\omega}^2}\phi_1. \tag{121}$$

To determine the constant M, N, we assume that the inner boundary is non-reflective, thus $N = 0$. For the outer boundary, we assume that the pressure perturbation vanishes, i.e., $\eta_1 = 0$, this determines M and eq. (A9) then becomes

$$\eta_1 = Q^{-1}G - \left[\frac{Q^{-1}G}{(D/r\sigma)^{1/2}Q^{-1/4}}\right]_{r_{out}} (D/r\sigma)^{1/2} Q^{-1/4} \exp(i \int_{r}^{r_{out}} Q^{1/2} dr). \tag{122}$$

A direct calculation using eq. (33) shows that the angular momentum flux carried by the wave is

$$F_1 = \pi \left(\frac{r\sigma G^2}{Q^{3/2} D}\right)_{r_{out}} = \pi \left(\frac{r\sigma D \phi_1^2}{h^4 \tilde{\omega}^4 Q^{3/2}}\right)_{r_{out}}. \tag{123}$$

Therefore, in this model, waves are mainly generated at the outer disk boundary, propagating inward, while the angular momentum is transferred outward.

8 DISCUSSION

Here we discuss several assumptions/issues related to our theory and how they might affect the results of the paper.

(i) *Radially Nonisothermal Disks.* In deriving the basic equation (29) for the disk perturbation, we have dropped several terms proportional to the radial gradient of the sound speed (see footnotes 1 and 2). It is easy to see that these terms vary on the lengthscale of r and do not introduce any singularity or turning point in our equation, therefore they do not affect any of our results concerning wave excitation/damping studied in §§4-7. However, a r-dependent sound speed gives rise to a nonzero $\partial\Omega/dz$, which can modify the structure of the perturbation equation near corotation. Indeed, if the (unperturbed) surface density σ and sound speed c profiles satisfy simple power-laws, $\sigma \propto r^{-\alpha}$ and $c \propto r^{-\beta}$, then the angular velocity profile in the disk is given by (Tanaka et al. 2002)

** The wavenumber k for the $n = m = 1$ mode (for Keplerian disks) is given by $k^2h^2 = (\omega/\Omega)^2(2\Omega - \omega)^2/(\Omega - \omega)^2$, which reduces to $k^2h^2 = (2\omega/\Omega)^2 \ll 1$ for $\omega < \Omega(r_{out}) \ll \Omega$. Thus the radial wavelength may be much larger than h and comparable to r, in which case the WKB solution is not valid.

$$\Omega = \Omega_K \left\{ 1 - \frac{1}{2}\left(\frac{h}{r}\right)^2 \left[\frac{3}{2} + \alpha + \beta \left(\frac{z^2}{h^2} + 1 \right) \right] \right\}, \tag{124}$$

where $\Omega_K(r)$ is the Keplerian angular velocity. For a thin disk, the deviation of $\Omega(r,z)$ from Ω_K is obviously very small. Nevertheless, if the z-dependence of Ω is taken into account, an additional term, $(-\beta mn\Omega D/r^2\tilde{\omega}^3)w_n$ should be be added to the left-hand-side of eq. (29)[††]. Obviously, this term does not affect waves near a Lindblad resonance and vertical resonance. Because of the strong $\tilde{\omega}^{-3}$ singularity at corotation (where $\tilde{\omega}=0$), one might suspect that our result on the $n \geq 1$ corotation resonance (see §6.2) may be affected (see Tanaka et al. 2002). In fact, we can show this is not the case. With the $\tilde{\omega}^{-3}$ term included, the perturbation equation near a $n \geq 1$ corotation resonance is modified from eq. (111) to

$$\frac{d^2\eta_n}{dx^2} + \frac{C}{x^2}\eta_n + \frac{C_1}{x^3}\eta_n = -\frac{C\phi_n}{x^2} - \frac{C_1\phi_n}{x^3}, \tag{125}$$

where

$$C_1 = -\frac{n\beta}{m^2}\left[\frac{\kappa^2\Omega}{r^3(d\Omega/dr)^3}\right]_{r_c}. \tag{126}$$

Since $C \sim (n/m^2)(r_c/h)^2 \gg 1$ while $C_1 \sim n\beta/m^2$, the new terms are important only for $|x| \lesssim \beta(h/r_c)^2$. Thus we expect that our solution, eq. (113), remains valid for $|x| \gg \beta(h/r_c)^2$. Indeed, the general solution of eq. (125) is

$$\eta_n = -\phi_n + Mx^{\frac{1}{2}}J_{i2\nu}(2C_1^{\frac{1}{2}}x^{-\frac{1}{2}}) + Nx^{\frac{1}{2}}J_{-i2\nu}(2C_1^{\frac{1}{2}}x^{-\frac{1}{2}}), \tag{127}$$

where $\nu = \sqrt{C - 1/4}$, and $J_{\pm 2i\nu}$ is the Bessel function (Abramowitz & Stegun 1964, p. 358). This solution approaches the form of eq. (113) for $|x| \gg \beta(h/r_c)^2$. Therefore, the analysis in §6.2 remains valid and our result on wave absorption at the $n \geq 1$ corotation resonance is unchanged. We conclude that while our theory is explicitly based on radially isothermal disks, our results remain valid when this condition breaks down.

(ii) *Vertical structure of disks.* Our theory is concerned with vertically isothermal disks, for which 3-dimensional perturbations can be decomposed into various Hermite components [eq. (15); see Tanaka et al. 2002]. It would be interesting to investigate if similar decomposition (with different basis functions) is possible for more general disk temperature profiles. To simplify our equations, we have also neglected stratification in our analysis [see eq. (8)]. In particular, vertical stratification gives rise to a local Brunt-Väisälä frequency of order $\Omega_\perp(z/h)^{1/2}$, and it is not clear to what extent such stratification will affect our results involving vertical fluid motion in the disk (see Lubow & Ogilvie 1998). This issue requires further study.

(iii) *Non-Keplerian Disks.* Although in this paper we have considered Keplerian disks (for which $\Omega = \kappa = \Omega_\perp$), extension to more general disks is not difficult. Indeed, since we have been careful to distinguish Ω, κ, $\Omega_\perp$ throughout the paper, most of our equations are valid when $\Omega \neq \kappa \neq \Omega_\perp$. The only exception is the $n=1$ Lindblad/vertical resonances studied in §4.2: Only for a Keplerian disk ($\Omega_\perp = \kappa$) is the $n=1$ vertical resonance degenerate with the Lindblad resonance, and such a combined Lindblad/vertical resonance needs special treatment. For a disk where the Lindblad resonance and $n=1$ vertical resonance are well separated, they must be treated separately, with the procedure similar to those given in §4.1 (for Lindblad resonances) or §5 (for vertical resonances). For a nearly Keplerian disk, with $|\Omega_\perp - \kappa|/\kappa \ll 1$, the LR (at r_L) and the $n=1$ VR (at r_V) are rather close, and the problem requires some consideration. Expanding eq. (40) around the Lindblad resonance, we find [cf. eq. (64)]

$$\frac{d^2}{dx^2}\eta_1 - \frac{1}{x}\frac{d}{dx}\eta_1 + b^2x(x-x_V)\eta_1 = \frac{\psi_1}{x} - \alpha_1 x, \tag{128}$$

where $x_V = (r_V - r_L)/r_L$ and α_1, b, ψ_1 are given by eq. (65). Obviously, solution (67) breaks down for $|x| \lesssim |x_V|$. For $bx_V^2 \ll 1$, or $|x_V| \ll b^{-1/2} \sim (h/r_L)^{1/2}$, the asymptotic solutions (73) and (74) remain valid and the angular momentum flux is unchanged. For $bx_V^2 \gtrsim 1$, the angular momentum flux expression has the same form as eq. (75) or (76) except that the pre-factor $(m\pi^2/2)$ may be changed by a factor of order unity.

(iv) *Nonlinear effect.* From the wave solutions we have derived in this paper, we see that the enthalpy or density perturbation of the disk is finite at various resonances. However, the azimuthal velocity perturbation can become singular at the corotation resonance (GT). Viscous and nonlinear effects may become important at the resonance and affect the derived torque formula. Therefore, linear, inviscid theory for the corotation resonance is incomplete even for a very small external potential. As has been pointed out by Balmforth & Korycansky (2001), and largely discussed in hydrodynamic stability theory (see Drazin & Reid 1981), critical layer may emerge at the resonance. This issue requires further study (see Ogilvie & Lubow 2003; Goldreich & Sari 2003).

[††] Nonzero $\partial\Omega/\partial z$ also gives rise to an additional "coupling" term, $\propto (\beta/\tilde{\omega}^3)\eta_{n+2}$. This can be neglected [see the discussion following eq. (29)].

9 CONCLUSION

In the paper we have studied the linear response of a 3D gaseous disk to a rigidly rotating external potential. The disk is assumed to be non-self-gravitating, geometrically thin and vertically isothermal. The external potential and the disk perturbation can be decomposed into various Fourier-Hermite components, each proportional to $H_n(z/h)\exp(im\theta - i\omega t)]$, characterized by the azimuthal index m and the vertical index n which specifies the number of nodes along the z-direction in the fluid density perturbation. We have derived analytical expressions for the various wave modes excited at Lindblad resonances and vertical resonances, and calculated the angular momentum fluxes associated with these waves and hence the torque on the disk from the external potential. We have also studied wave damping and angular momentum transfer at corotation resonances. For wave modes that involves only 2D motion ($n = 0$), our general formulae reduce to the standard result of Goldreich & Tremaine (1979).

Our main results on wave excitation/damping can be most conveniently summarized using the wave propagation diagram (Figs. 1-2) which follows from the dispersion relation [eq. (35)]. In 2D disks, waves are excited only at the inner and outer Lindblad resonances, and propagate away from the corotation. By contrast, in 3D disks, additional channels of wave generation open up through vertical resonances, and waves can propagate into corotation and where angular momenta are deposited. Irrespective of the direction of propagation of the excited waves, the torque on the disk is positive for waves generated at outer Linblad or vertical resonances and negative at inner resonances.

Our paper contains a number of analytical results which are obtained for the first time. A guide to the key equations are as follows: (i) *Lindblad resonances:* For the $n = 0$ and $n \geq 2$ modes, the wave amplitudes excited at the resonances are given by eqs. (58)-(59), the associated angular momentum fluxes eqs. (60) and (62) and the torque on the disk eq. (63); for $n = 1$, the Lindblad resonance and vertical resonance coincide for a Keplerian disk, the corresponding equations are (73)-(74), (75)-(76) and (77). (ii) *Vertical resonances:* For $n \geq 2$, the waves amplitudes excited at the vertical resonances are given by eqs. (82)-(83), the angular momentum fluxes eqs. (84)-(85) and the torque on the disk eq. (86). (iii) *Corotation resonances:* For $n = 0$, waves cannot propagate around the corotation region, but a torque is delivered to the disk at corotation. An improved expression for the torque is given by eq. (109), which reduces to the standard Goldreich-Tremaine result (94) in the $h/r \to 0$ limit. For $n > 0$, waves can propagate into the corotation. The angular momentum flux deposited to the disk at corotation is given by eq. (116) or (119), depending on the incident wave amplitude.

The last paragraph refers to waves excited by a prograde-rotating potential (with pattern speed $\Omega_p = \omega/m > 0$). It is of interest to note that for $m < \sqrt{n}$, vertical resonant excitations exist for a retrograde-rotating potential (with $\Omega_p < 0$, i.e., the perturber rotates in the direction opposite to the disk rotation): The excited wave has an amplitude given by eq. (87) and angular momentum flux given by eq. (88).

Even without any resonance, waves can be excited at disk boundaries. An example is discussed in §7.

An interesting finding of our paper is that for a given potential component ϕ_n with $n \geq 1$, vertical resonances are much more efficient [by a factor of order $(r/h)^2$] than Lindblad resonances in transferring angular momentum to the disk. Whether vertical resonances can compete with $n = 0$ Lindblad resonances depend on the relative values of ϕ_n ($n \geq 1$) and ϕ_0. Since we expect $\phi_n \propto (h/r)^n$, the angular momentum transfer through the $n = 1$ vertical resonance may be as important as the $n = 0$ Lindblad resonace when considering the perturbation of a circumstellar disk by a planet in an inclined orbit. We plan to investigate this and other related issues discussed in §8 in the future.

APPENDIX A: SOLUTIONS AWAY FROM RESONANCES

In the region away from any of the resonances, we only need to retain in eq. (29) the first and second derivative terms as well as the terms $\propto h^{-2}$. Thus for $n > 0$, eq. (29) reduces to

$$\frac{d^2}{dr^2}\eta_n + \left(\frac{d}{dr}\ln\frac{r\sigma}{D}\right)\frac{d}{dr}\eta_n + Q\eta_n = G, \tag{A1}$$

where for $n > 0$,

$$Q = -\frac{D(\tilde{\omega}^2 - n\Omega_\perp^2)}{h^2\tilde{\omega}^2\Omega_\perp^2}, \tag{A2}$$

$$G = -\frac{nD}{h^2\tilde{\omega}^2}\phi_n, \qquad (n > 0). \tag{A3}$$

For $n = 0$, all the potential terms in eq. (29) must kept, thus

$$Q = -\frac{D}{h^2\Omega_\perp^2}, \tag{A4}$$

$$G = \left[-\frac{d^2}{dr^2} - \left(\frac{d}{dr}\ln\frac{r\sigma}{D}\right)\frac{d}{dr} + \frac{2m\Omega}{r\tilde{\omega}}\left(\frac{d}{dr}\ln\frac{\Omega\sigma}{D}\right) + \frac{m^2}{r^2}\right]\phi_0$$

$$+\frac{2\mu}{r}\left(\frac{d}{dr}-\frac{d}{dr}\ln\frac{D}{\sigma}+\frac{2m\Omega}{r\tilde{\omega}}\right)\phi_2, \qquad (n=0). \tag{A5}$$

Clearly, $Q=k^2$ gives the WKB dispersion relation (35), and $|Q|\sim h^{-2}$. After making a transformation of the variable,

$$y=(r\sigma/D)^{1/2}\eta_n, \tag{A6}$$

and using $|Q|\gg 1/r^2$, eq. (A1) reduces to

$$\frac{d^2y}{d^2r}+Qy=(r\sigma/D)^{1/2}G. \tag{A7}$$

In the wave-propagating region ($Q>0$), the Liouville-Green or WKB approximation gives two independent solutions to the homogeneous equation of (A7) (e.g., Olver 1974)

$$y_1=Q^{-1/4}\exp(-i\int^r Q^{1/2}dr), \quad y_2=Q^{-1/4}\exp(i\int^r Q^{1/2}dr). \tag{A8}$$

A particular solution to eq. (A7) can be written asymptotically, owing to the large parameter Q, as $y=Q^{-1}(r\sigma/D)^{1/2}G$, Thus the general solution to eq. (A1) is

$$\eta_n=Q^{-1}G+(D/r\sigma)^{1/2}Q^{-1/4}\left[M\exp(-i\int^r Q^{1/2}dr)+N\exp(i\int^r Q^{1/2}dr)\right], \tag{A9}$$

where the two constants M and N are determined by boundary conditions. The boundary conditions may be imposed at the true disk boundary, or by the requirement to match the wave coming from a resonance.

The the evanescent region ($Q<0$), the general solution to eq. (A1) can be obtained in a similar way:

$$\eta_n=Q^{-1}G+(D/r\sigma)^{1/2}|Q|^{-1/4}\left[M\exp(-\int^r |Q|^{1/2}dr)+N\exp(\int^r |Q|^{1/2}dr)\right]. \tag{A10}$$

APPENDIX B: AN EXAMPLE OF WAVE EXCITATION AND ABSORPTION

Here we give an example of the global solution of wave excitation at a Lindblad/vertical resonance, wave propagation, and wave absorption at corotation. For definiteness, we consider the $n=1$ case, and assume that the wave excited at the L/VR (see §4.2) does not suffer any damping as it propagates toward the corotation radius. The wave excited from the outer L/VR at $r=r_{OL}$ is given by eq. (74) and can be rewritten as

$$\eta_1=-i\sqrt{\frac{\pi}{2}}\,e^{i\pi/4}\left(\frac{\Omega_\perp\phi_1}{h^{1/2}|dD/dr|^{1/2}}\right)_{r_{OL}}\exp\left[-i\frac{1}{2}\left|\frac{dD/dr}{h\Omega_\perp^2}\right|_{r_{OL}}(r-r_{OL})^2\right]. \tag{B1}$$

For the region between the corotation and the outer L/VR, $r_c<r<r_{OL}$, the general solution is given by eq. (A9). Note that in this region, the group velocity c_g has opposite sign as the phase velocity (see Figs. 1-2). Keeping only the inward-propagating wave term, we have

$$\eta_1=N(D/r\sigma)^{1/2}Q^{-1/4}\exp(i\int_{r_0}^r Q^{1/2}dr), \tag{B2}$$

where r_0 is a fiducial radius ($r_c<r_0<r_{OL}$). Matching (B2) with (B1) as $r\to r_{OL}$ gives

$$N=-i\sqrt{\frac{\pi}{2}}\,e^{i\pi/4}\left[\left(\frac{r\sigma}{|dD/dr|}\right)^{1/2}h^{-1}\phi_1\right]_{r_{OL}}\exp(-i\int_{r_0}^{r_{OL}}Q^{1/2}dr). \tag{B3}$$

Matching (B2) with $\eta_1=A_+x^{1/2}e^{i\nu\ln x}$ [see eq. (114)] as $r\to r_c$ [or $x=(r-r_c)/r_c\to 0+$] yields

$$|A_+|=\sqrt{\frac{\pi m}{2}}\left(\frac{h\Omega|d\Omega/dr|}{\sigma}\right)_{r_c}^{1/2}\left[\left(\frac{r\sigma}{|dD/dr|}\right)^{1/2}h^{-1}\phi_1\right]_{r_{OL}}. \tag{B4}$$

The angular momentum flux associated the wave at $r=r_c+$ is then [see eq. (116)]

$$F_1(r=r_c+)=-\pi\left(\frac{\sigma}{\Omega h|d\Omega/dr|}\right)_{r_c}|A_+|^2=-\frac{\pi^2 m}{2}\left(\frac{r\sigma\phi_1^2}{h^2|dD/dr|}\right)_{r_{OL}}. \tag{B5}$$

That is, the angular momentum absorbed at $r=r_c+$ is $-F_1(r=r_c+)$. Not surprisingly, this is exactly equal to the inward angular momentum flux transferred away from the OL/VR, i.e., $-F_1(r<r_{OL/VR})$ [see eq. (76)].

We can similarly show that the angular momentum transferred by the waves excited at the inner Lindblad resonance and propagating to the corotation is absorbed at corotation, as well as the waves themselves.

ACKNOWLEDGMENTS

We thank the referee for useful comments which improved this paper. H.Z. thanks the hospitality of the Astronomy department at Cornell University, where this work was carried out. D.L. thanks IAS (Princeton), CITA (Toronto), TIARA (Taiwan), KITP (Santa Barbara) and NAOC (Beijing) and Tsinghua University (Beijing) for extended visits during the period of this research. This work was supported in part by the Fok Ying Dung Education Foundation, by the NSF grant AST 0307252 and NASA grant NAG 5-12034.

REFERENCES

Abramowitz, M., Stegun, I.A., 1964, Handbook of Mathematical Functions, Dover, New York
Artymowicz, P., 1993, ApJ, 419, 155
Artymowicz, P., 1994, ApJ, 423, 581
Balmforth, N.J., Korycansky, D.G., 2001, MNRAS, 326, 883
Bate, M.R., Ogilvie, G.I., Lubow, S.H., & Pringle, J.E. 2002, MNRAS, 332, 575
Booker, J. & Bretherton, F.P., 1967, J. Fluid Mech., 27, 513
Drazin, P.G., Reid, W.H., 1981, Hydrodynamic Stability, Cambridge University Press, Cambridge
Erdélyi, A., et al, 1953, Higher Transcendental Functions, Vol.1, McGraw-Hill, New York
Goldreich, P. & Sari, R. 1993, ApJ, 585, 1024
Goldreich, P. & Tremaine, S. 1978, Icarus, 34, 240
Goldreich, P. & Tremaine, S. 1979, ApJ, 233, 857 (GT)
Goldreich, P. & Tremaine, S. 1980, ApJ, 241, 425
Kato, S. 2001, PASJ, 53, 1
Kato, S. 2003, PASJ, 55, 257
Korycansky, D.G., Pollack, J.B.,1993, Icarus, 102, 150
Li, L.-X., Goodman, J., & Narayan, R. 2003, ApJ, 593, 980.
Lin, D.N.C., Papaloizou, J. 1979, MNRAS, 186, 799
Lubow, S.H, 1981, ApJ, 245, 274
Lubow, S.H., Ogilvie, G.I., 1998, ApJ, 504, 983
Lubow, S.H., Pringle, J.E., 1993, ApJ, 409, 360
Masset, F.S., Papaloizou, J.C.B., 2003, ApJ, 588, 494
Meyer-Vernet, N., & Sicardy, B. 1987, Icarus, 69, 157
Ogilvie, G.I., 2002, MNRAS, 331, 1053
Ogilvie, G.I., & Lubow, S.H. 2003, ApJ, 587, 398
Okazaki, A., Kato, S., & Fukue, J. 1987, PASJ, 39, 457
Olver, F.W.J. 1974, Asymptotics and Special Functions, Academic Press, New York
Papaloizou, J.C.B., & Lin, D.C. 1995, ApJ, 438, 841
Shu, F.H., Yuan, C., Lissauer, J.J., 1985, ApJ, 291, 356
Takeuchi, T., & Miyama, S.M. 1998, PASJ, 50, 141
Tanaka, H., Takeuchi, T., & Ward, W.R. 2002, ApJ, 565, 1257
Tanaka, H., & Ward, W.R. 200, ApJ, 602, 388
Terquem, C. 1998, ApJ, 509, 819
Ward, W.R. 1986, Icarus, 67, 164
Ward, W.R. 1988, Icarus, 73, 330
Ward, W.R., 1997, ApJ, 482, L211
Ward, W.R., Hahn, J.M., 2003, ApJ, 125, 3389
Wong, R., 2001, Asymptotic Approximations of integrals, SIAM, Philadelphia

This paper has been produced using the Royal Astronomical Society/Blackwell Science LaTeX style file.